ITUPublications
Recommendations

International Telecommunication Union
Radiocommunication Sector

Recommendation ITU-R P.452-18

(08/2023)

P Series: Radiowave propagation

Prediction procedure for the evaluation of interference between stations on the surface of the Earth at frequencies above about 100 MHz

Foreword

The role of the Radiocommunication Sector is to ensure the rational, equitable, efficient and economical use of the radio-frequency spectrum by all radiocommunication services, including satellite services, and carry out studies without limit of frequency range on the basis of which Recommendations are adopted.

The regulatory and policy functions of the Radiocommunication Sector are performed by World and Regional Radiocommunication Conferences and Radiocommunication Assemblies supported by Study Groups.

Policy on Intellectual Property Right (IPR)

ITU-R policy on IPR is described in the Common Patent Policy for ITU-T/ITU-R/ISO/IEC referenced in Resolution ITU-R 1. Forms to be used for the submission of patent statements and licensing declarations by patent holders are available from http://www.itu.int/ITU-R/go/patents/en where the Guidelines for Implementation of the Common Patent Policy for ITU-T/ITU-R/ISO/IEC and the ITU-R patent information database can also be found.

Series of ITU-R Recommendations

(Also available online at https://www.itu.int/publ/R-REC/en)

Series	Title
BO	Satellite delivery
BR	Recording for production, archival and play-out; film for television
BS	Broadcasting service (sound)
BT	Broadcasting service (television)
F	Fixed service
M	Mobile, radiodetermination, amateur and related satellite services
P	**Radiowave propagation**
RA	Radio astronomy
RS	Remote sensing systems
S	Fixed-satellite service
SA	Space applications and meteorology
SF	Frequency sharing and coordination between fixed-satellite and fixed service systems
SM	Spectrum management
SNG	Satellite news gathering
TF	Time signals and frequency standards emissions
V	Vocabulary and related subjects

Note: *This ITU-R Recommendation was approved in English under the procedure detailed in Resolution ITU-R 1.*

Electronic Publication
Geneva, 2023

RECOMMENDATION ITU-R P.452-18

Prediction procedure for the evaluation of interference between stations on the surface of the Earth at frequencies above about 100 MHz

(Question ITU-R 208/3)

(1970-1974-1978-1982-1986-1992-1994-1995-1997-1999-2001-2003-2005-2007-2009-2013-2015-2021-2023)

Scope

This Recommendation contains a prediction method for the evaluation of interference between stations on the surface of the Earth at frequencies from about 100 MHz to 50 GHz, accounting for both clear-air and hydrometeor scattering interference mechanisms.

Keywords

Interference, Ducting, Tropospheric scatter, Diffraction, Hydrometeor Scattering, Digital Data Products

Abbreviations/Glossary

Amsl	Above mean sea level
IDWM	ITU Digitized World Map
LoS	Line-of-sight

Related ITU Recommendations, Reports

Recommendation ITU-R S.465

Recommendation ITU-R S.580

Recommendation ITU-R P.676

Recommendation ITU-R F.699

Recommendation ITU-R P.837

Recommendation ITU-R P.838

Recommendation ITU-R P.839

Recommendation ITU-R P.1058

Recommendation ITU-R P.1144

Recommendation ITU-R F.1245

Recommendation ITU-R F.1336

NOTE – The latest revision/edition of the Recommendation/Report should be used.

The ITU Radiocommunication Assembly,

considering

a) that due to congestion of the radio spectrum, frequency bands must be shared between different terrestrial services, between systems in the same service and between systems in the terrestrial and Earth-space services;

b) that for the satisfactory coexistence of systems sharing the same frequency bands, interference prediction procedures are needed that are accurate and reliable in operation and acceptable to all parties concerned;

c) that propagation predictions are applied in interference prediction procedures which are often required to meet "worst-month" performance and availability objectives;

d) that prediction methods are required for application to all types of paths in all areas of the world,

recommends

that the interference prediction procedure given in Annex 1 should be used for the evaluation of the available propagation loss over unwanted signal paths between stations on the surface of the Earth for frequencies above about 100 MHz.

Annex 1

TABLE OF CONTENTS

Page

1 Introduction

Congestion of the radio-frequency spectrum has made necessary the sharing of many frequency bands between different radio services, and between the different operators of similar radio services. In order to ensure the satisfactory coexistence of the terrestrial and Earth-space systems involved, it is important to be able to predict with reasonable accuracy the interference potential between them, using propagation predictions and models which are acceptable to all parties concerned, and which have demonstrated accuracy and reliability.

Many types and combinations of interference path may exist between stations on the surface of the Earth, and between these stations and stations in space, and prediction methods are required for each situation. This Annex addresses one of the more important sets of interference problems, i.e. those situations where there is a potential for interference between radio stations located on the surface of the Earth.

The models contained within this Recommendation work from the assumption that the interfering transmitter and the interfered-with receiver both operate within the surface layer of atmosphere. Use of exceptionally large antenna heights to model operations such as aeronautical systems is not appropriate for these models. The prediction procedure has been tested for radio stations operating in the frequency range of about 0.1 GHz to 50 GHz.

The models within this Recommendation are designed to calculate propagation losses not exceeded for time percentages over the range $0.001 \leq p \leq 50\%$. This assumption does not imply the maximum loss will be at $p = 50\%$.

The method includes a complementary set of propagation models which ensure that the predictions embrace all the significant interference propagation mechanisms that can arise. Methods for analysing the radio-meteorological and topographical features of the path are provided so that predictions can be prepared for any practical interference path falling within the scope of the procedure up to a distance limit of 10 000 km.

2 Interference propagation mechanisms

Interference may arise through a range of propagation mechanisms whose individual dominance depends on climate, radio frequency, time percentage of interest, distance and path topography. At any one time a single mechanism or more than one may be present. The principal interference propagation mechanisms are as follows:

– *Line-of-sight* (Fig. 1): The most straightforward interference propagation situation is when a line-of-sight transmission path exists under normal (i.e. well-mixed) atmospheric conditions. However, an additional complexity can come into play when subpath diffraction causes a slight increase in signal level above that normally expected. Also, on all but the shortest paths (i.e. paths longer than about 5 km) signal levels can often be significantly enhanced for short periods of time by multipath and focusing effects resulting from atmospheric stratification (see Fig. 2).

– *Diffraction* (Fig. 1): Beyond line-of-sight (LoS) and under normal conditions, diffraction effects generally dominate wherever significant signal levels are to be found. For services where anomalous short-term problems are not important, the accuracy to which diffraction can be modelled generally determines the density of systems that can be achieved. The diffraction prediction capability must have sufficient utility to cover smooth-earth, discrete obstacle and irregular (unstructured) terrain and clutter situations.

– *Tropospheric scatter* (Fig. 1): This mechanism defines the “background” interference level for longer paths (e.g. more than 100-150 km) where the diffraction field becomes very weak. However, except for a few special cases involving sensitive receivers or very high power

interferers (e.g. radar systems), interference via troposcatter will be at too low a level to be significant.

FIGURE 1

Long-term interference propagation mechanisms

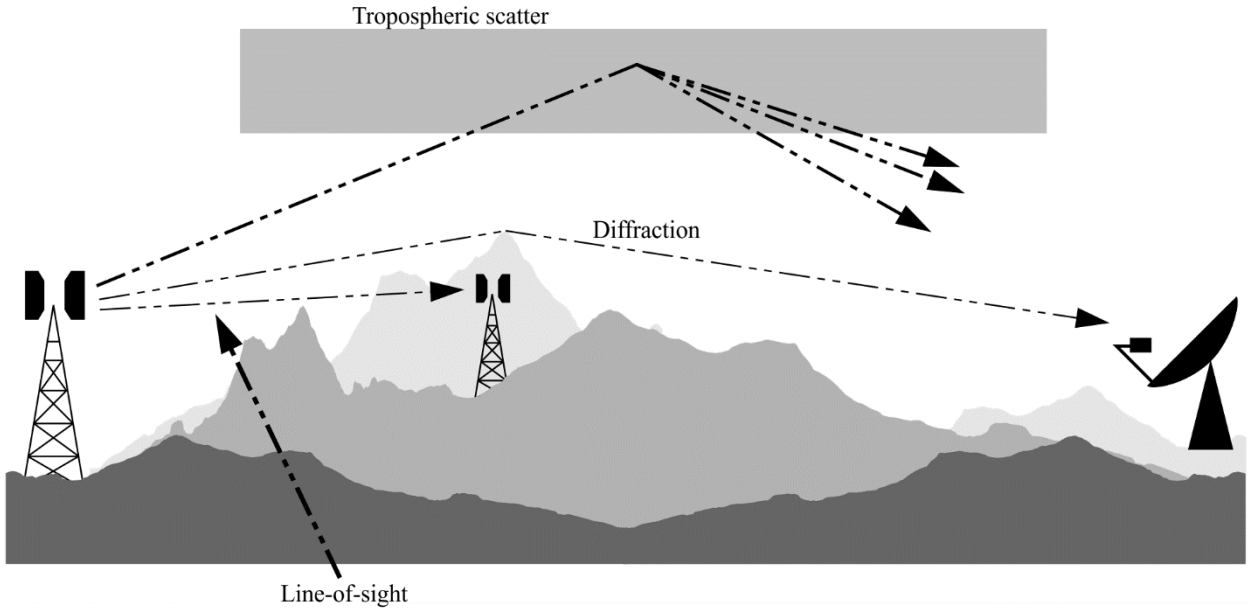

– *Surface ducting* (Fig. 2): This is the most important short-term propagation mechanism that can cause interference over water and in flat coastal land areas, and can give rise to high signal levels over long distances (more than 500 km over the sea). Such signals can exceed the equivalent “free-space” level under certain conditions.

FIGURE 2

Anomalous (short-term) interference propagation mechanisms

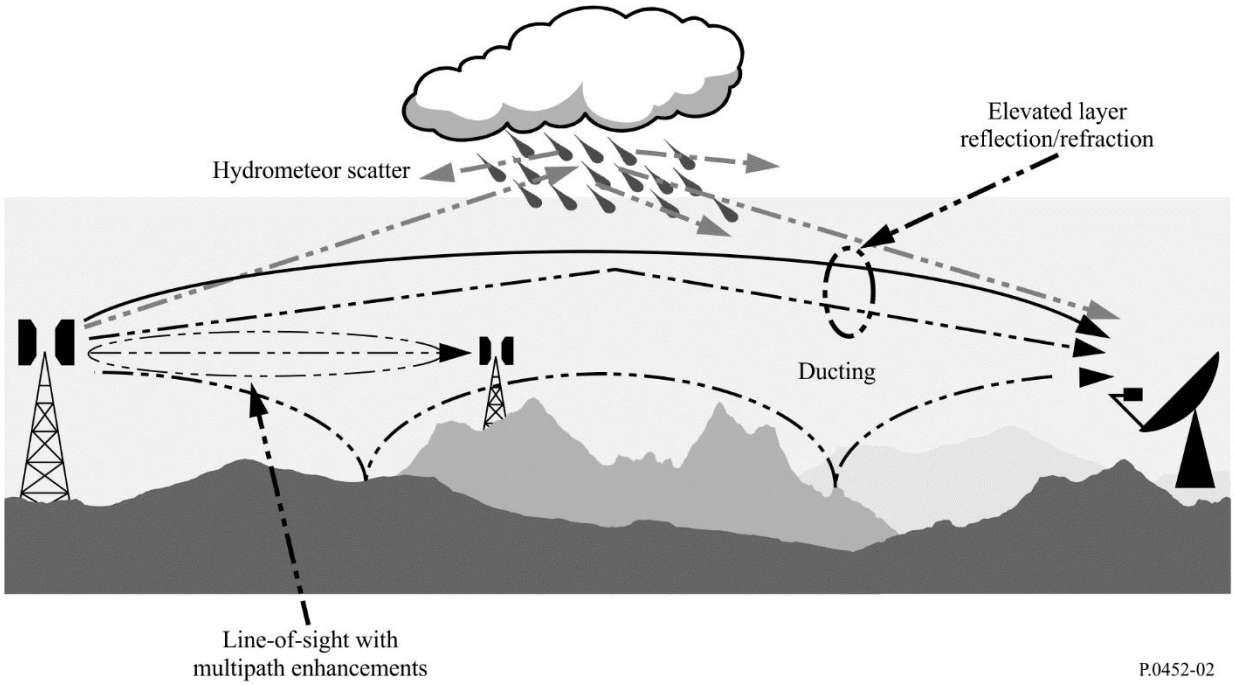

– *Elevated layer reflection and refraction* (Fig. 2): The treatment of reflection and/or refraction from layers at heights up to a few hundred metres is of major importance as these mechanisms enable signals to overcome the diffraction loss of the terrain very effectively under favourable path geometry situations. Again the impact can be significant over quite long distances (up to 250-300 km).

– *Hydrometeor scatter* (Fig. 2): Hydrometeor scatter can be a potential source of interference between terrestrial link transmitters and earth stations because it may act virtually omnidirectionally, and can therefore have an impact off the great-circle interference path. However, the interfering signal levels are quite low and do not usually represent a significant problem.

A basic problem in interference prediction (which is indeed common to all tropospheric prediction procedures) is the difficulty of providing a unified consistent set of practical methods covering a wide range of distances and time percentages; i.e. for the real atmosphere in which the statistics of dominance by one mechanism merge gradually into another as meteorological and/or path conditions change. Especially in these transitional regions, a given level of signal may occur for a total time percentage which is the sum of those in different mechanisms. The approach in this procedure has been to define completely separate methods for clear-air and hydrometeor-scatter interference prediction, as described in §§ 4 and 5 respectively.

The clear-air method consists of separate models for diffraction, ducting/layer-reflection, and troposcatter. All three are applied for every case, irrespective of whether a path is LoS or transhorizon. The results are then combined into an overall prediction using a blending technique that ensures for any given path distance and time percentage that the signal enhancement in the equivalent notional line-of-sight model is the highest attainable.

3 Clear-air interference prediction

3.1 General comments

Although the clear-air method is implemented by three separate models, the results of which are then blended, the procedure takes account of four basic types of propagation mechanism:

– line-of-sight (including signal enhancements due to multipath and focusing effects);

– diffraction (embracing smooth-earth, irregular terrain, clutter and sub-path cases);

– tropospheric scatter;

– anomalous propagation (ducting and layer reflection/refraction).

3.2 Deriving a prediction

3.2.1 Outline of the procedure

The steps required to achieve a prediction are as follows:

Step 1: Input data

The basic input data required for the procedure is given in Table 1. All other information required is derived from these basic data during the execution of the procedure.

TABLE 1

Basic input data

Parameter	Preferred resolution	Description
f	0.01	Frequency (GHz)
p	0.001	Required time percentage(s) for which the calculated basic transmission loss is not exceeded
φ_t, φ_r	0.001	Latitude of station (degrees)
ψ_t, ψ_r	0.001	Longitude of station (degrees)
h_{tg}, h_{rg}	1	Antenna centre height above ground level (m)
h_{ts}, h_{rs}	1	Antenna centre height above mean sea level (m)
G_t, G_r	0.1	Antenna gain in the direction of the horizon along the great-circle interference path (dBi)
Pol	N/A	Signal, e.g. vertical or horizontal

NOTE 1 – For the interfering and interfered-with stations:

t: interferer

r: interfered-with station.

Polarization in Table 1 is not a parameter with a numerical value. The information is used in § 4.2.2.1 in connection with equations (30a), (30b) and (31).

Step 2: Selecting average year or worst-month prediction

The choice of annual or "worst-month" predictions is generally dictated by the quality (i.e. performance and availability) objectives of the interfered-with radio system at the receiving end of the interference path. As interference is often a bidirectional problem, two such sets of quality objectives may need to be evaluated in order to determine the worst-case direction upon which the minimum permissible basic transmission loss needs to be based. In the majority of cases the quality objectives will be couched in terms of a percentage "of any month", and hence worst-month data will be needed.

The propagation prediction models predict the annual distribution of basic transmission loss. For average year predictions the percentages of time p, for which particular values of basic transmission loss are not exceeded, are used directly in the prediction procedure. If average worst-month predictions are required, the annual equivalent time percentage, p, of the worst-month time percentage, p_w, must be calculated for the path centre latitude φ using:

$$p = 10^{\left(\frac{\log_{10}(p_W)+\log_{10}(G_L)-0.186\omega-0.444}{0.816+0.078\omega}\right)} \quad (1)$$

where:

ω: fraction of the path over water (see Table 4).

$$G_L = \begin{cases} \sqrt{1.1 + |\cos 2\varphi|^{0.7}} & \text{for } |\varphi| \le 45° \\ \sqrt{1.1 - |\cos 2\varphi|^{0.7}} & \text{for } |\varphi| > 45° \end{cases} \quad (1a)$$

If necessary, the value of p must be limited such that $12\,p \ge p_w$.

Note that the latitude φ (degrees) is deemed to be positive in the Northern Hemisphere.

The calculated result will then represent the basic transmission loss for the required worst-month time percentage, p_w%.

Step 3: Radiometeorological data

The prediction procedure employs three radio-meteorological parameters to describe the variability of background and anomalous propagation conditions at the different locations around the world.

– ΔN (N-units/km), the average radio-refractivity lapse-rate through the lowest 1 km of the atmosphere, provides the data upon which the appropriate effective Earth radius can be calculated for path profile and diffraction obstacle analysis. Note that ΔN is a positive quantity in this procedure.

– β_0 (%), the time percentage for which refractivity lapse-rates exceeding 100 N-units/km can be expected in the first 100 m of the lower atmosphere, is used to estimate the relative incidence of fully developed anomalous propagation at the latitude under consideration. The value of β_0 to be used is that appropriate to the path centre latitude.

– N_0 (N-units), the sea-level surface refractivity, is used only by the troposcatter model as a measure of location variability of the troposcatter scatter mechanism. As the scatter path calculation is based on a path geometry determined by annual or worst-month values of ΔN, there is no additional need for worst-month values of N_0. The correct values of ΔN and N_0 are given by the path-centre values as derived from the appropriate maps.

Point incidence of anomalous propagation, β_0 (%), for the path centre location is determined using:

$$\beta_0 = \begin{cases} 10^{-0.015|\varphi| + 1.67}\,\mu_1\,\mu_4 & \% \quad \text{for } |\varphi| \le 70^\circ \\ 4.17\,\mu_1\,\mu_4 & \% \quad \text{for } |\varphi| > 70^\circ \end{cases} \tag{2}$$

where:

φ: path centre latitude (degrees).

The parameter μ_1 depends on the degree to which the path is over land (inland and/or coastal) and water, and is given by:

$$\mu_1 = \left[10^{\frac{-d_{tm}}{16 - 6.6\,\tau}} + \left[10^{-(0.496 + 0.354\,\tau)} \right]^5 \right]^{0.2} \tag{3}$$

where the value of μ_1 shall be limited to $\mu_1 \le 1$,

with:

$$\tau = \left[1 - e^{-\left(4.12 \times 10^{-4} \times d_{lm}^{2.41} \right)} \right] \tag{3a}$$

where:

d_{tm}: longest continuous land (inland + coastal) section of the great-circle path (km);

d_{lm}: longest continuous inland section of the great-circle path (km).

The radioclimatic zones to be used for the derivation of d_{tm} and d_{lm} are defined in Table 2.

$$\mu_4 = \begin{cases} 10^{(-0.935 + 0.0176|\varphi|)\log_{10}\mu_1} & \text{for } |\varphi| \le 70^\circ \\ 10^{0.3\log_{10}\mu_1} & \text{for } |\varphi| > 70^\circ \end{cases} \tag{4}$$

TABLE 2

Radio-climatic zones

Zone type	Code	Definition
Coastal land	A1	Coastal land and shore areas, i.e. land adjacent to the sea up to an altitude of 100 m relative to mean sea or water level, but limited to a distance of 50 km from the nearest sea area. Where precise 100 m data are not available an approximate value, i.e. 300 ft, may be used
Inland	A2	All land, other than coastal and shore areas defined as "coastal land" above
Sea	B	Seas, oceans and other large bodies of water (i.e. covering a circle of at least 100 km in diameter)

Large bodies of inland water

A "large" body of inland water, to be considered as lying in Zone B, is defined as one having an area of at least 7 800 km^2, but excluding the area of rivers. Islands within such bodies of water are to be included as water within the calculation of this area if they have elevations lower than 100 m above the mean water level for more than 90% of their area. Islands that do not meet these criteria should be classified as land for the purposes of the water area calculation.

Large inland lake or wet-land areas

Large inland areas of greater than 7 800 km^2 which contain many small lakes or a river network should be declared as "coastal" Zone A1 by administrations if the area comprises more than 50% water, and more than 90% of the land is less than 100 m above the mean water level.

Climatic regions pertaining to Zone A1, large inland bodies of water and large inland lake and wetland regions, are difficult to determine unambiguously. Therefore, administrations are invited to register with the ITU Radiocommunication Bureau (BR) those regions within their territorial boundaries that they wish identified as belonging to one of these categories. In the absence of registered information to the contrary, all land areas will be considered to pertain to climate Zone A2.

For maximum consistency of results between administrations the calculations of this procedure should be based on the ITU Digitized World Map (IDWM) which is available from the BR. If all points on the path are at least 50 km from the sea or other large bodies of water, then only the inland category applies.

If the zone information is stored in successive points along the radio path, it should be assumed that changes occur midway between points having different zone codes.

Effective Earth radius

The median effective Earth radius factor k_{50} for the path is determined using:

$$k_{50} = \frac{157}{157 - \Delta N} \tag{5}$$

Assuming the average physical Earth radius of $a = 6\,371$ km, the median value of effective Earth radius a_e can be determined from:

$$a_e = k_{50} a \quad \text{km} \tag{6a}$$

The effective Earth radius exceeded for β_0% time, a_β, is given by:

$$a_\beta = k_\beta a \quad \text{km} \tag{6b}$$

where $k_\beta = 3.0$ is an estimate of the effective Earth radius factor exceeded for β_0% time.

A general effective earth radius, a_p, will be set to a_e for 50% time and to a_β for β_0% time in §§ 4.2.1 and 4.2.2.

Step 4: Radio path profile

The path profiles used in the method described below require path-specific data for terrain (bare-earth) and path-specific clutter (ground cover) categories along the path. The method includes:

– the construction of a terrain profile using actual terrain heights;

– based on the clutter categories, the addition of representative clutter heights to the terrain profile.

If this method is used to calculate diffraction loss using the terrain profile without clutter, the diffraction loss will be under-estimated in cluttered environments, as opposed to combined representation of terrain and clutter. This method has been developed and validated against digital terrain data, by combining digital terrain data with statistical representative clutter categories as opposed to direct use of surface-height data, where heights include clutter with no explicit distinction between terrain and clutter. It is important to note that diffraction loss may be over-estimated if terrain profiles include surface-height data. If accurate surface-height data are available, other techniques such as 3-D ray tracing, which would include the effect of diffraction around buildings, could be explored to arrive at a more accurate estimation of the propagation losses.

A profile for the radio path is required for the application of the propagation prediction method. The profile should include information on terrain (bare earth) heights and clutter (ground cover) heights along the path.

It is convenient to store information in three arrays each having the same number of values, $n + 1$, as follows:

d_i: distance from transmitter of i-th profile point (km) (6c)

h_i: terrain height of the i-th profile point above sea level (m) (6d)

$$g_i = \begin{cases} h_i + \text{representative clutter height of } i\text{-th profile point (m)} & \text{for } i = 1, \ldots, n-1 \\ h_0 & \text{for } i = 0 \\ h_n & \text{for } i = n \end{cases} \quad (6e)$$

where:

i: 0, 1, 2, ..., n = index of the profile point

$n + 1$: number of profile points.

There must be at least one intermediate profile point between the transmitter and the receiver. Thus, n must satisfy $n \geq 2$. Such a small number of points is appropriate only for short paths, less than of the order of 1 km.

Note that the first profile point is at the transmitter. Thus, d_0 is zero and h_0 is the terrain height at the transmitter in metres above sea level. Similarly, the n-th profile point is at the receiver. Thus, d_n is the path length in km and h_n is the terrain height at the receiver in metres above sea level.

No specific distance between profile points is given. Assuming that profiles are extracted from digital terrain elevation and ground cover (clutter) datasets, a suitable spacing will typically be similar to the point spacing of the source datasets of similar resolution to each other. The profile points are not required to be equally spaced, but it is desirable that they are at a similar spacing for the whole profile and no less than of the order of 30 m.

The arrays used for the calculations comprise distances, d_i, terrain heights, h_i, as given by equation (6d) and terrain heights with representative clutter heights added, g_i, as given by equation (6e). The representative clutter height should not be added to the terrain heights at the transmitter and the

receiver and if the distance from the transmitter or the receiver is less than 50 m. Thus, g_0 is the terrain height at the transmitter in metres above sea level and g_n is the terrain height at the receiver in metres above sea level and g_i is the terrain height in metres above sea level for all the points at a distance from transmitter or receiver less than 50 m.

The "representative clutter height" referred to in equation (6e) concerns statistical height information associated with ground cover classification, such as vegetation and buildings, i.e. a single height value assigned to each ground cover /clutter class. Adding representative clutter heights to a profile is based on the assumption that the heights h_i represent the bare surface of the Earth. If the radio path passes over woodland or urbanization where diffraction or sub-path obstruction occurs, in general the effective profile height will be higher because the radio signal will travel over the clutter. Thus, a more suitable representation of the profile can be obtained by adding representative heights to account for the clutter.

The appropriate addition is not necessarily physical, such as rooftop heights in the case of buildings. Where gaps exist between clutter objects, as seen by the radio wave, some energy may travel between rather than over them. In this situation the presence of clutter is expected to increase diffraction loss, but not by as much as raising the profile to the physical clutter height.

This applies particularly to high-rise urban areas. Categories such as "dense urban" or "high-rise urban" tend to be associated with building heights of 30 metres or more. But some high-rise areas have large spaces between the tall buildings, and it is possible for low-loss paths to exist passing around them, rather than over the roofs. Smaller values of representative heights rather than the physical clutter heights may be appropriate in such cases.

At the other extreme, even in areas classified as "open" or "rural" it is unusual for the ground to be completely bare, that is, free of any objects which might add to propagation losses. Thus, small values of representative heights, rather than zero, might be appropriate in many cases.

Thus, representative clutter height depends not only on the typical physical height of clutter objects but also on the horizontal spacing of objects and the gaps between them. There is no accepted standard as to what a clutter category, such as "urban", represents in physical terms in different countries. Where available, representative clutter height information based on local clutter height statistics or other sources should be used. Table 3 suggests default values for representative clutter heights which may be used in the absence of region/country specific information.

TABLE 3

Default representative clutter height values

Clutter category	**Representative clutter height (m)**
	Add to profile of equation (6e) for $i = 1$ to $n - 1$
Water/sea	0
Open/rural	0
Suburban	10
Urban/trees/forest	15
Dense urban	20

Values for a number of path-related parameters necessary for the calculations, as indicated in Table 4, must be derived via an initial analysis of the path profile based on the value of a_e given by

equation (6a). Information on the derivation, construction and analysis of the path profile is given in Attachment 2 to Annex 1.

TABLE 4

Parameter values to be derived from the path profile analysis

Parameter	Description
d	Great-circle path distance (km)
d_{lt}, d_{lr}	Distance from the transmit and receive antennas to their respective horizons (km).
θ_t, θ_r	For a transhorizon path, transmit and receive horizon elevation angles respectively (mrad). For a LoS path, each is set to the elevation angle to the other terminal
θ	Path angular distance (mrad)
h_{ts}, h_{rs}	Antenna centre height above mean sea level (m)
h_{te}, h_{re}	Effective heights of antennas above the terrain (m) for the ducting/layer-reflection model (see Attachment 2 to Annex 1 for definitions). Note that the same parameter names are used for effective heights in the diffraction model, but h_{te} and h_{re} have different definitions in the diffraction model. See equations (39a) and (39b)
d_b	Aggregate length of the path sections over water (km)
ω	Fraction of the total path over water: $\omega = d_b / d$ (7) where d is the great-circle distance (km) calculated using equation (134). For totally overland paths: $\omega = 0$
$d_{ct,cr}$	Distance over land from the transmit and receive antennas to the coast along the great-circle interference path (km). Set to zero for a terminal on a ship or sea platform

4 Clear-air propagation models

Basic transmission loss, L_b (dB), not exceeded for the required annual percentage time, p, is evaluated as described in the following sub-sections.

4.1 Line-of-sight propagation (including short-term effects)

The following should be evaluated for both LoS and transhorizon paths.

Basic transmission loss due to free-space propagation and attenuation by atmospheric gases:

$$L_{bfsg} = 92.4 + 20 \log_{10} f + 20 \log_{10} d_{fs} + A_g(d_{fs}) \quad \text{dB} \quad (8)$$

where:

f: frequency (GHz)

d_{fs}: distance between the transmit and receive antennas (km):

$$d_{fs} = \sqrt{d^2 + \left(\frac{h_{ts} - h_{rs}}{1\,000}\right)^2} \quad (8a)$$

d: great-circle path distance (km)

h_{ts}: transmit antenna height above sea level (m)

h_{rs}: receive antenna height above sea level (m)

A_g: total gaseous absorption (dB):

$$A_g(d_{fs}) = [\gamma_0 + \gamma_w(\rho)] \cdot d_{fs} \quad \text{dB} \tag{9}$$

where:

γ_o, $\gamma_w(\rho)$: specific attenuation due to dry air and water vapour, respectively, and are found from the equations in Recommendation ITU-R P.676

ρ: water vapour density:

$$\rho = 7.5 + 2.5\omega \quad \text{g/m}^3 \tag{9a}$$

ω: fraction of the total path over water.

Corrections for multipath and focusing effects at p and β_0 percentage times:

$$E_{sp} = 2.6\,[1 - \exp(-0.1\,\{d_{lt} + d_{lr}\})]\,\log_{10}(p/50) \quad \text{dB} \tag{10a}$$

$$E_{s\beta} = 2.6\,[1 - \exp(-0.1\,\{d_{lt} + d_{lr}\})]\,\log_{10}(\beta_0/50) \quad \text{dB} \tag{10b}$$

Basic transmission loss not exceeded for time percentage, p%, due to LoS propagation:

$$L_{b0p} = L_{bfsg} + E_{sp} \quad \text{dB} \tag{11}$$

Basic transmission loss not exceeded for time percentage, β_0%, due to LoS propagation (regardless of whether or not the path is actually LoS):

$$L_{b0\beta} = L_{bfsg} + E_{s\beta} \quad \text{dB} \tag{12}$$

4.2 Diffraction

The time variability of the excess loss due to the diffraction mechanism is assumed to be the result of changes in bulk atmospheric radio refractivity lapse rate, i.e. as the time percentage p reduces, the effective Earth radius factor $k(p)$ is assumed to increase. This process is considered valid for $\beta_0 \le p \le 50\%$. For time percentages less than β_0 signal levels are dominated by anomalous propagation mechanisms rather than by the bulk refractivity characteristics of the atmosphere. Thus diffraction loss not exceeded for $p < \beta_0\%$ is assumed to be the same as for $p = \beta_0\%$ time.

Taking this into account, in the general case where $p < 50\%$, the diffraction calculation must be performed twice, first for the median effective Earth-radius factor k_{50} (equation (5)) and second for the limiting effective Earth-radius factor k_β equal to 3. This second calculation gives an estimate of diffraction loss not exceeded for β_0% time, where β_0 is given by equation (2).

The diffraction loss L_{dp} not exceeded for p% time, for $0.001\% \le p \le 50\%$, is then calculated using a limiting or interpolation procedure described in § 4.2.4.

The diffraction model calculates the following quantities required in § 4.5:

L_{dp}: diffraction loss not exceeded for p% time

L_{bd50}: median basic transmission loss associated with diffraction

L_{bd}: basic transmission loss associated with diffraction not exceeded for p% time.

The diffraction loss is calculated by the combination of a method based on the Bullington construction and spherical-Earth diffraction. The Bullington part of the method is an expansion of the basic Bullington construction to control the transition between free-space and obstructed conditions. This part of the method is used twice: for the actual path profile, and for a zero-height smooth profile with modified antenna heights referred to as effective antenna heights. The same effective antenna heights are also used to calculate the spherical-Earth diffraction loss. The final result is obtained as a

combination of three losses calculated as above. For a perfectly smooth path, the final diffraction loss will be the output of the spherical-Earth model.

This method provides an estimate of diffraction loss for all types of paths, including over-sea or over-inland or coastal land, and irrespective of whether the land is smooth or rough, and whether LoS or transhorizon.

This method also makes extensive use of an approximation to the single knife-edge diffraction loss as a function of the dimensionless parameter, ν, given by:

$$J(\nu) = 6.9 + 20\log_{10}\left(\sqrt{(\nu - 0.1)^2 + 1} + \nu - 0.1\right) \quad (13)$$

Note that $J(-0.78) \approx 0$, and this defines the lower limit at which this approximation should be used. $J(\nu)$ is set to zero for $\nu < -0.78$.

The overall diffraction calculation is described in the subsections as follows:

Section 4.2.1 describes the Bullington part of the diffraction method. For each diffraction calculation for a given effective Earth radius this is used twice. On the second occasion, the antenna heights are modified and all profile heights are zero.

Section 4.2.2 describes the spherical-Earth part of the diffraction model. This is used with the same antenna heights as for the second use of the Bullington part in § 4.2.1.

Section 4.2.3 describes how the methods in §§ 4.2.1 and 4.2.2 are used in combination to perform the complete diffraction calculation for a given effective Earth radius. Due to the manner in which the Bullington and spherical-Earth parts are used, the complete calculation has come to be known as the "delta-Bullington" model.

Section 4.2.4 describes the complete calculation for diffraction loss not exceeded for a given percentage time *p*%.

4.2.1 The Bullington part of the diffraction calculation

In the following equations, slopes are calculated in m/km relative to the baseline joining sea level at the transmitter to sea level at the receiver. The distance and height (including representative clutter height) of the *i*-th profile point are d_i kilometres and g_i metres above mean sea level respectively, *i* takes values from 0 to *n* where $n + 1$ is the number of profile points, and the complete path length is *d* kilometres. For convenience the terminals at the start and end of the profile are referred to as transmitter and receiver, with heights in m above sea level, h_{ts} and h_{rs}, respectively. Effective Earth curvature C_e km^{-1} is given by $1/a_p$ where a_p is effective earth radius in kilometres. Wavelength in metres is represented by λ. Values to be used for a_p are given in § 4.2.4.

Care is needed close to the terminals to ensure that the addition of representative heights of local clutter does not cause an unrealistic increase in the horizon elevation angles as seen by each antenna.

Find the intermediate profile point with the highest slope of the line from the transmitter to the point.

$$S_{tim} = \max\left[\frac{g_i + 500 C_e d_i (d - d_i) - h_{ts}}{d_i}\right] \quad \text{m/km} \quad (14)$$

where the profile index *i* takes values from 1 to $n - 1$.

Calculate the slope of the line from transmitter to receiver assuming a LoS path:

$$S_{tr} = \frac{h_{rs} - h_{ts}}{d} \quad \text{m/km} \quad (15)$$

Two cases must now be considered.

Case 1. Path is LoS

If $S_{tim} < S_{tr}$ the path is LoS.

Find the intermediate profile point with the highest diffraction parameter ν:

$$\nu_{\max} = \max\left\{\left[g_i + 500C_e d_i(d-d_i) - \frac{h_{ts}(d-d_i)+h_{rs}d_i}{d}\right]\sqrt{\frac{0.002d}{\lambda d_i(d-d_i)}}\right\} \quad (16)$$

where the profile index i takes values from 1 to $n-1$.

In this case, the knife-edge loss for the Bullington point is given by:

$$L_{uc} = J\left(\nu_{\max}\right) \quad \text{dB} \quad (17)$$

where the function J is given by equation (13) for ν_b greater than −0.78, and is zero otherwise.

Case 2. Path is transhorizon

If $S_{tim} \geq S_{tr}$ the path is transhorizon.

Find the intermediate profile point with the highest slope of the line from the receiver to the point.

$$S_{rim} = \max\left[\frac{g_i+500C_e d_i(d-d_i)-h_{rs}}{d-d_i}\right] \quad \text{m/km} \quad (18)$$

where the profile index i takes values from 1 to $n-1$.

Calculate the distance of the Bullington point from the transmitter:

$$d_{bp} = \frac{h_{rs}-h_{ts}+S_{rim}d}{S_{tim}+S_{rim}} \quad \text{km} \quad (19)$$

Calculate the diffraction parameter, ν_b, for the Bullington point

$$\nu_b = \left[h_{ts} + S_{tim}d_{bp} - \frac{h_{ts}\left(d-d_{bp}\right)+h_{rs}d_{bp}}{d}\right]\sqrt{\frac{0.002d}{\lambda d_{bp}\left(d-d_{bp}\right)}} \quad (20)$$

In this case, the knife-edge loss for the Bullington point is given by:

$$L_{uc} = J\left(\nu_b\right) \quad \text{dB} \quad (21)$$

For L_{uc} calculated using either equation (17) or (21), Bullington diffraction loss for the path is now given by:

$$L_{bull} = L_{uc} + [1 - \exp(-L_{uc}/6)](10+0.02\,d) \quad \text{dB} \quad (22)$$

4.2.2 Spherical-Earth diffraction loss

The spherical-Earth diffraction loss for antenna heights h_{te} and h_{re} (m), L_{dsph}, is calculated as follows.

Calculate the marginal LoS distance for a smooth path:

$$d_{los} = \sqrt{2a_p}\cdot\left(\sqrt{0.001h_{te}} + \sqrt{0.001h_{re}}\right) \quad \text{km} \quad (23)$$

Values to be used for a_p are given in § 4.2.4. Effective antenna heights h_{te} and h_{re} are defined in equations (39a) and (39b).

If $d \geq d_{los}$ calculate diffraction loss using the method in § 4.2.2.1 below for $a_{dft} = a_p$ to give L_{dft}, and set L_{dsph} equal to L_{dft}. No further spherical-Earth diffraction calculation is necessary.

Otherwise continue as follows:

Calculate the smallest clearance height between the curved-Earth path and the ray between the antennas, h_{se}, given by:

$$h_{se} = \frac{\left(h_{te} - 500\frac{d_{se1}^2}{a_p}\right)d_{se2} + \left(h_{re} - 500\frac{d_{se2}^2}{a_p}\right)d_{se1}}{d} \quad \text{m} \tag{24}$$

where:

$$d_{se1} = \frac{d}{2}(1 + b) \quad \text{km} \tag{25a}$$

$$d_{se2} = d - d_{se1} \quad \text{km} \tag{25b}$$

$$b = 2\sqrt{\frac{m+1}{3m}}\cos\left\{\frac{\pi}{3} + \frac{1}{3}\arccos\left(\frac{3c}{2}\sqrt{\frac{3m}{(m+1)^3}}\right)\right\} \tag{25c}$$

where the arccos function returns an angle in radians.

$$c = \frac{h_{te} - h_{re}}{h_{te} + h_{re}} \tag{25d}$$

$$m = \frac{250d^2}{a_p(h_{te} + h_{re})} \tag{25e}$$

Calculate the required clearance for zero diffraction loss, h_{req}, given by:

$$h_{req} = 17.456\sqrt{\frac{d_{se1} \cdot d_{se2} \cdot \lambda}{d}} \quad \text{m} \tag{26}$$

If $h_{se} > h_{req}$ the spherical-Earth diffraction loss L_{dsph} is zero. No further spherical-Earth diffraction calculation is necessary.

Otherwise continue as follows:

Calculate the modified effective earth radius, a_{em}, which gives marginal LoS at distance d given by:

$$a_{em} = 500\left(\frac{d}{\sqrt{h_{te}} + \sqrt{h_{re}}}\right)^2 \quad \text{km} \tag{27}$$

Use the method in § 4.2.2.1 for $a_{dft} = a_{em}$ to give L_{dft}.

If L_{dft} is negative, the spherical-Earth diffraction loss, L_{dsph}, is zero, and no further spherical-Earth diffraction calculation is necessary.

Otherwise continue as follows:

Calculate the spherical-Earth diffraction loss by interpolation:

$$L_{dsph} = \left[1 - h_{se}/h_{req}\right]L_{dft} \quad \text{dB} \tag{28}$$

4.2.2.1 First-term part of spherical-Earth diffraction loss

This sub-section gives the method for calculating spherical-Earth diffraction using only the first term of the residue series. It forms part of the overall diffraction method described in § 4.2.2 above to give the first-term diffraction loss, L_{dft}, for a given value of effective Earth radius a_{dft}. The value of a_{dft} to use is given in § 4.2.2.

Set terrain electrical properties typical for land, with relative permittivity $\varepsilon_r = 22.0$ and conductivity $\sigma = 0.003$ S/m and calculate L_{dft} using equations (30) to (37) and call the result $L_{dftland}$.

Set terrain electrical properties typical for sea, with relative permittivity $\varepsilon_r = 80.0$ and conductivity $\sigma = 5.0$ S/m and calculate L_{dft} using equations (30) to (37) and call the result L_{dftsea}.

First-term spherical diffraction loss is now given by:

$$L_{dft} = \omega L_{dftsea} + (1 - \omega) L_{dftland} \quad \text{dB} \tag{29}$$

where ω is the fraction of the path over sea.

Start of calculation to be performed twice, as described above:

Normalized factor for surface admittance for horizontal and vertical polarization.

$$K_H = 0.036\left(a_{dft} f\right)^{-1/3} \left[(\varepsilon_r - 1)^2 + (18\sigma/f)^2\right]^{-1/4} \quad \text{(horizontal)} \tag{30a}$$

and:

$$K_V = K_H \left[\varepsilon_r^2 + (18\,\sigma / f)^2 \right]^{1/2} \quad \text{(vertical)} \tag{30b}$$

If the polarization vector contains both horizontal and vertical components, e.g. circular or slant, decompose it into horizontal and vertical components, calculate each separately starting from equations (30a) and (30b) and combine the results by a vector sum of the field amplitude. In practice this decomposition will generally be unnecessary because above 300 MHz a value of 1 can be used for β_{dft} in equation (31).

Calculate the Earth ground/polarization parameter:

$$\beta_{dft} = \frac{1 + 1.6K^2 + 0.67K^4}{1 + 4.5K^2 + 1.53K^4} \tag{31}$$

where K is K_H or K_V according to polarization.

Normalized distance:

$$X = 21.88\,\beta_{dft} \left(\frac{f}{a_{dft}^2} \right)^{1/3} d \tag{32}$$

Normalized transmitter and receiver heights:

$$Y_t = 0.9575\,\beta_{dft} \left(\frac{f^2}{a_{dft}} \right)^{1/3} h_{te} \tag{33a}$$

$$Y_r = 0.9575\,\beta_{dft} \left(\frac{f^2}{a_{dft}} \right)^{1/3} h_{re} \tag{33b}$$

Calculate the distance term given by:

$$F_X = \begin{cases} 11 + 10\log_{10}(X) - 17.6X & \text{for } X \geq 1.6 \\ -20\log_{10}(X) - 5.6488X^{1.425} & \text{or } X < 1.6 \end{cases} \tag{34}$$

Define a function of normalized height given by:

$$G(Y_{t/r}) = \begin{cases} 17.6\left(B_{t/r} - 1.1\right)^{0.5} - 5\log_{10}\left(B_{t/r} - 1.1\right) - 8 & \text{for } B_{t/r} > 2 \\ 20\log_{10}\left(B_{t/r} + 0.1B_{t/r}^{3}\right) & \text{otherwise} \end{cases} \quad (35)$$

where:

$$B_t = \beta_{dft} Y_t \quad (36a)$$

$$B_r = \beta_{dft} Y_r \quad (36b)$$

If $G(Y)$ is less than $2 + 20\log_{10} K$, then limit $G(Y)$ such that $G(Y) = 2 + 20\log_{10} K$.

The first-term spherical-Earth diffraction loss is now given by:

$$L_{dft} = -F_X - G(Y_t) - G(Y_r) \quad \text{dB} \quad (37)$$

4.2.3 Complete 'delta-Bullington' diffraction loss model

Use the method in § 4.2.1 for the path profile heights (g_i) and antenna heights. Set the resulting Bullington diffraction loss for the actual path, $L_{bulla}=L_{bull}$ as given by equation (22).

Use the method in § 4.2.1 for a second time, with all profile heights, g_i, set to zero, and modified antenna heights given by:

$$h'_{ts} = h_{ts} - h_{std} \quad \text{m (amsl)} \quad (38a)$$

$$h'_{rs} = h_{rs} - h_{srd} \quad \text{m (amsl)} \quad (38b)$$

where the smooth-Earth heights at transmitter and receiver, h_{std} and h_{srd}, are given in § 5.1.6.3 of Attachment 2. Set the resulting Bullington diffraction loss for this smooth path, $L_{bulls}=L_{bull}$ as given by equation (22).

Use the method in § 4.2.2 to calculate the spherical-Earth diffraction loss L_{dsph} for the actual path length d (km) and with:

$$h_{te} = h'_{ts} \quad \text{m (amsl)} \quad (39a)$$

$$h_{re} = h'_{rs} \quad \text{m (amsl)} \quad (39b)$$

Diffraction loss for the general path is now given by:

$$L_d = L_{bulla} + \max\{L_{dsph} - L_{bulls}, 0\} \quad \text{dB} \quad (40)$$

4.2.4 The diffraction loss not exceeded for *p*% of the time

Use the method in § 4.2.3 to calculate diffraction loss L_d for effective Earth radius $a_p=a_e$ as given by equation (6a). Set median diffraction loss $L_{d50} = L_d$.

If $p = 50\%$ the diffraction loss not exceeded for p% time, L_{dp}, is given by L_{d50}, and this completes the diffraction calculation.

If $p < 50\%$ continue as follows.

Use the method in § 4.2.3 to calculate diffraction loss L_d for effective Earth radius $a_p = a_\beta$ as given in equation (6b). Set diffraction loss not exceeded for β_0% time $L_{d\beta} = L_d$.

The application of the two possible values of effective Earth radius factor is controlled by an interpolation factor, F_i, based on the normal distribution of diffraction loss over the range $\beta_0\% \le p < 50\%$ given by:

$$F_i = \frac{I\left(\frac{p}{100}\right)}{I\left(\frac{\beta_0}{100}\right)} \qquad \text{for } 50\% > p > \beta_0\% \tag{41a}$$

$$= 1 \qquad \text{for } \beta_0\% \geq p \tag{41b}$$

where $I(x)$ is the inverse complementary cumulative normal function. An approximation for $I(x)$ which may be used with confidence for $x < 0.5$ is given in Attachment 3 to Annex 1.

The diffraction loss, L_{dp}, not exceeded for p% time, is now given by:

$$L_{dp} = L_{d50} + F_i \, (L_{d\beta} - L_{d50}) \qquad \text{dB} \tag{42}$$

where L_{d50} and $L_{d\beta}$ are defined above, and F_i is defined by equations (41a) and (41b), depending on the values of p and β_0.

The median basic transmission loss associated with diffraction, L_{bd50}, is given by:

$$L_{bd50} = L_{bfsg} + L_{d50} \qquad \text{dB} \tag{43}$$

where L_{bfsg} is given by equation (8).

The basic transmission loss associated with diffraction not exceeded for p% time is given by:

$$L_{bd} = L_{b0p} + L_{dp} \qquad \text{dB} \tag{44}$$

where L_{b0p} is given by equation (11).

4.3 Tropospheric scatter

NOTE 1 – At time percentages much below 50%, it is difficult to separate the true tropospheric scatter mode from other secondary propagation phenomena which give rise to similar propagation effects. The "tropospheric scatter" model adopted in this Recommendation is therefore an empirical generalization of the concept of tropospheric scatter which also embraces these secondary propagation effects. This allows a continuous consistent prediction of basic transmission loss over the range of time percentages p from 0.001% to 50%, thus linking the ducting and layer reflection model at the small time percentages with the true "scatter mode" appropriate to the weak residual field exceeded for the largest time percentage.

NOTE 2 – This troposcatter prediction model has been derived for interference prediction purposes and is not appropriate for the calculation of propagation conditions above 50% of time affecting the performance aspects of trans-horizon radio-relay systems.

The basic transmission loss due to troposcatter, L_{bs} (dB) not exceeded for any time percentage, p, below 50%, is given by:

$$L_{bs} = 190 + L_f + 20 \ \log_{10} d + 0.573\theta - 0.15 \, N_0 + L_c + A_g - 10.1[-\log_{10} \ (p/50)]^{0.7} \ \text{dB} \tag{45}$$

where:

L_f: frequency dependent loss:

$$L_f = 25 \log_{10} f - 2.5 \left[\log_{10} (f / 2)\right]^2 \qquad \text{dB} \tag{45a}$$

L_c: aperture to medium coupling loss (dB):

$$L_c = 0.051 \cdot \mathrm{e}^{0.055(G_t + G_r)} \qquad \text{dB} \tag{45b}$$

N_0: path centre sea-level surface refractivity from the maps in Attachment 1 to Annex 1

A_g: gaseous absorption derived from equation (9) using $\rho = 3$ g/m^3 for the whole path length.

4.4 Ducting/layer reflection

The prediction of the basic transmission loss, L_{ba} (dB) occurring during periods of anomalous propagation (ducting and layer reflection) is based on the following function:

$$L_{ba} = A_f + A_d(p) + A_g \quad \text{dB} \tag{46}$$

where:

A_f: total of fixed coupling losses between the antennas and the anomalous propagation structure within the atmosphere:

$$A_f = 102.45 + 20 \log_{10} f + 20 \log_{10}(d_{lt} + d_{lr}) + A_{lf} + A_{st} + A_{sr} + A_{ct} + A_{cr} \quad \text{dB} \tag{47}$$

A_{lf}: empirical correction to account for the increasing attenuation with wavelength inducted propagation:

$$A_{lf}(f) = 45.375 - 137.0 \cdot f + 92.5 \cdot f^2 \quad \text{dB} \quad \text{if } f < 0.5 \text{ GHz} \tag{47a}$$

$$A_{lf}(f) = 0.0 \text{ dB} \quad \text{otherwise}$$

A_{st}, A_{sr}: site-shielding diffraction losses for the interfering and interfered-with stations respectively:

$$A_{st,sr} = \begin{cases} 20 \log_{10}\left[1 + 0.361\theta''_{t,r}\left(f \cdot d_{lt,lr}\right)^{1/2}\right] + 0.264\theta''_{t,r} f^{1/3} & \text{dB for } \theta''_{t,r} > 0 \text{ mrad} \\ 0 & \text{dB for } \theta''_{t,r} \le 0 \text{ mrad} \end{cases} \tag{48}$$

where:

$$\theta''_{t,r} = \theta_{t,r} - 0.1\, d_{lt,lr} \quad \text{mrad} \tag{48a}$$

A_{ct}, A_{cr}: over-sea surface duct coupling corrections for the interfering and interfered-with stations respectively:

$$A_{ct,cr} = -3\, e^{-0.25\, d_{ct,cr}^2} \left[1 + \tanh\ (0.07(50 - h_{ts,rs}))\right] \quad \text{dB} \quad \text{for } \omega \ge 0.75$$

$$d_{ct,cr} \le d_{lt,lr} \tag{49}$$

$$d_{ct,cr} \le 5 \text{ km}$$

$$A_{ct,cr} = 0 \quad \text{dB} \quad \text{for all other conditions} \tag{49a}$$

It is useful to note the limited set of conditions under which equation (49) is needed.

$A_d(p)$: time percentage and angular-distance dependent losses within the anomalous propagation mechanism:

$$A_d(p) = \gamma_d \cdot \theta' + A(p) \quad \text{dB} \tag{50}$$

where:

γ_d: specific attenuation:

$$\gamma_d = 5 \times 10^{-5}\, a_e\, f^{1/3} \quad \text{dB/mrad} \tag{51}$$

θ': angular distance (corrected where appropriate (via equation (52a)) to allow for the application of the site shielding model in equation (48)):

$$\theta' = \frac{10^3 d}{a_e} + \theta'_t + \theta'_r \quad \text{mrad} \tag{52}$$

$$\theta'_{t,r} = \begin{cases} \theta_{t,r} & \text{for } \theta_{t,r} \le 0.1\, d_{lt,lr} \quad \text{mrad} \\ 0.1\, d_{lt,lr} & \text{for } \theta_{t,r} > 0.1\, d_{lt,lr} \quad \text{mrad} \end{cases} \tag{52a}$$

$A(p)$: time percentage variability (cumulative distribution):

$$A(p) = -12 + (1.2 + 3.7 \times 10^{-3} d) \log_{10}\left(\frac{p}{\beta}\right) + 12\left(\frac{p}{\beta}\right)^{\Gamma} \tag{53}$$

$$\Gamma = \frac{1.076}{(2.0058 - \log_{10}\beta)^{1.012}} \times e^{-(9.51 - 4.8\log_{10}\beta + 0.198(\log_{10}\beta)^2) \times 10^{-6} \cdot d^{1.13}} \tag{53a}$$

$$\beta = \beta_0 \cdot \mu_2 \cdot \mu_3 \quad \% \tag{54}$$

μ_2: correction for path geometry:

$$\mu_2 = \left[\frac{500}{a_e} \frac{d^2}{\left(\sqrt{h_{te}} + \sqrt{h_{re}}\right)^2} \right]^{\alpha} \tag{55}$$

The value of μ_2 shall not exceed 1.

Effective antenna heights h_{te} and h_{re} are defined in equation (156).

$$\alpha = -0.6 - \varepsilon \cdot 10^{-9} \cdot d^{3.1} \cdot \tau \tag{55a}$$

where:

ε = 3.5

τ: is defined in equation (3a)

and the value of α shall not be allowed to reduce below –3.4.

μ_3: correction for terrain roughness:

$$\mu_3 = \begin{cases} 1 & \text{for } h_m \le 10 \text{ m} \\ \exp\left[-4.6 \times 10^{-5} (h_m - 10)(43 + 6 d_I)\right] & \text{for } h_m > 10 \text{ m} \end{cases} \tag{56}$$

$$d_I = \min(d - d_{lt} - d_{lr}, 40) \quad \text{km} \tag{57}$$

A_g: total gaseous absorption determined from equations (9) and (9a).

The remaining terms have been defined in Tables 1 and 2 and Attachment 2 to Annex 1.

4.5 The overall prediction

The following procedure should be applied to the results of the foregoing calculations for all paths.

Calculate an interpolation factor, F_j, to take account of slope parameters:

$$F_j = 1.0 - 0.5\left(1.0 + \tanh\left(3.0\ \xi \frac{(S_{tim} - S_{tr})}{\Theta}\right)\right) \tag{58}$$

where:

ξ: adjustable parameter currently set to 0.8

$(S_{tim} - S_{tr})$: slope parameters defined in equations (14) and (15) except to use h_i instead of g_i in equation (14)

Θ: adjustable parameter currently set to 0.3 mrad.

Calculate an interpolation factor, F_k, to take account of the great circle path distance:

$$F_k = 1.0 - 0.5\left(1.0 + \tanh\left(3.0\,\kappa\,\frac{(d - d_{sw})}{d_{sw}}\right)\right) \tag{59}$$

where:

d: great circle path length (km) (defined in Table 4)

d_{sw}: fixed parameter determining the distance range of the associated blending, set to 20

κ: fixed parameter determining the blending slope at the ends of the range, set to 0.5.

Calculate a notional minimum basic transmission loss, L_{minb0p} (dB) associated with LoS propagation and over-sea sub-path diffraction.

$$L_{\min b0p} = \begin{cases} L_{b0p} + (1-\omega)L_{dp} & \text{for } p < \beta_0 \\ L_{bd50} + (L_{b0\beta} + (1-\omega)L_{dp} - L_{bd50}) \cdot F_i & \text{for } p \geq \beta_0 \end{cases} \quad \text{dB} \tag{60}$$

where:

L_{b0p}: notional LoS basic transmission loss not exceeded for p% time, given by equation (11)

$L_{b0\beta}$: notional LoS basic transmission loss not exceeded for β% time, given by equation (12)

L_{dp}: diffraction loss not exceeded for p% time, calculated using the method in § 4.2

F_i: diffraction interpolation factor, given by equation (41).

Calculate a notional minimum basic transmission loss, L_{minbap} (dB), associated with LoS and transhorizon signal enhancements:

$$L_{minbap} = \eta \ln\left(\exp\left(\frac{L_{ba}}{\eta}\right) + \exp\left(\frac{L_{b0p}}{\eta}\right)\right) \quad \text{dB} \tag{61}$$

where:

L_{ba}: ducting/layer reflection basic transmission loss not exceeded for p% time, given by equation (46)

L_{b0p}: notional line-of-sight basic transmission loss not exceeded for p% time, given by equation (11)

η = 2.5.

Calculate a notional basic transmission loss, L_{bda} (dB), associated with diffraction and LoS or ducting/layer-reflection enhancements:

$$L_{bda} = \begin{cases} L_{bd} & \text{for } L_{minbap} > L_{bd} \\ L_{minbap} + (L_{bd} - L_{minbap})F_k & \text{for } L_{minbap} \leq L_{bd} \end{cases} \quad \text{dB} \tag{62}$$

where:

L_{bd}: basic transmission loss for diffraction not exceeded for p% time from equation (44)

F_k: interpolation factor given by equation (59) according the value of the great-circle path distance, d.

Calculate a modified basic transmission loss, L_{bam} (dB), which takes diffraction and LoS or ducting/layer-reflection enhancements into account:

$$L_{bam} = L_{bda} + \left(L_{\min b0p} - L_{bda}\right) F_j \quad \text{dB} \tag{63}$$

Calculate the final basic transmission loss not exceeded for p% time, L_b (dB), as given by:

$$L_b = -5 \log_{10}(10^{-0.2 L_{bs}} + 10^{-0.2 L_{bam}}) \quad \text{dB} \tag{64}$$

4.6 Calculation of transmission loss

The method described in §§ 4.1 to 4.5 above provides the basic transmission loss between the two stations. In order to calculate the signal level at one station due to interference from the other it is necessary to know the transmission loss, which takes account of the antenna gains of the two stations in the direction of the radio (i.e. interference) path between them. When the arrival angle of radio waves is known, the antenna gain in the direction of that arrival angle may be used.

The following procedure provides a method for the calculation of transmission loss between two terrestrial stations. As intermediate steps in the method, it also provides formulae for the calculation of the great-circle path length and angular distance based on the stations' geographic coordinates, as opposed to the derivations of these quantities from the path profile, as assumed in Table 4.

Calculate the angle subtended by the path at the centre of the Earth, δ, from the stations' geographic coordinates using:

$$\delta = \arccos(\sin(\varphi_t) \sin(\varphi_r) + \cos(\varphi_t) \cos(\varphi_r) \cos(\psi_t - \psi_r)) \quad \text{rad} \tag{65}$$

The great circle distance, d, between the stations is:

$$d = 6\,371 \cdot \delta \quad \text{km} \tag{66}$$

Calculate the bearing (azimuthal direction clockwise from true North) from station t to station r using:

$$\alpha_{tr} = \arccos(\{\sin(\varphi_r) - \sin(\varphi_t) \cos(\delta)\}/\sin(\delta) \cos(\varphi_t)) \quad \text{rad} \tag{67}$$

Having implemented equation (67), if $\psi_t - \psi_r > 0$ then:

$$\alpha_{tr} = 2\pi - \alpha_{tr} \quad \text{rad} \tag{68}$$

Calculate the bearing from station r to station t, α_{rt}, by symmetry from equations (67) and (68).

Next, assume that the main beam (boresight) direction of station t is (ε_t, α_t) in (elevation, bearing), while the main beam direction of station r is (ε_r, α_r). To obtain the elevation angles of the radio (i.e. interference) path at stations t and r, ε_{pt} and ε_{pr}, respectively, it is necessary to distinguish between line-of-sight and trans-horizon paths. For example, for line-of-sight paths:

$$\varepsilon_{pt} = \frac{h_r - h_t}{d} - \frac{d}{2a_e} \quad \text{rad} \tag{69a}$$

and:

$$\varepsilon_{pr} = \frac{h_t - h_r}{d} - \frac{d}{2a_e} \quad \text{rad} \tag{69b}$$

where h_t and h_r are the heights of the stations above mean sea level (km), while for trans-horizon paths, the elevation angles are given by their respective horizon angles:

$$\varepsilon_{pt} = \frac{\theta_t}{1\,000} \quad \text{rad} \tag{70a}$$

and:

$$\varepsilon_{pr} = \frac{\theta_r}{1\,000} \quad \text{rad} \tag{70b}$$

Note that the radio horizon angles, θ_t and θ_r (mrad), are first introduced in Table 4 and are defined in §§ 5.1.1 and 5.1.3, respectively, of Attachment 2 to Annex 1.

To calculate the off-boresight angles for stations *t* and *r*, χ_t and χ_r, respectively, in the direction of the interference path at stations *t* and *r*, it is recommended to use:

$$\chi_t = \arccos(\cos(\varepsilon_t)\cos(\varepsilon_{pt})\cos(\alpha_{tr} - \alpha_t) + \sin(\varepsilon_t)\sin(\varepsilon_{pt})) \tag{71a}$$

and:

$$\chi_r = \arccos(\cos(\varepsilon_r)\cos(\varepsilon_{pr})\cos(\alpha_{rt} - \alpha_r) + \sin(\varepsilon_r)\sin(\varepsilon_{pr})) \tag{71b}$$

Using their respective off-boresight angles, obtain the antenna gains for stations *t* and *r*, G_t and G_r, respectively (dB). If the actual antenna radiation patterns are not available, the variation of gain with off-boresight angle may be obtained from the information in Recommendation ITU-R S.465.

To obtain the transmission loss, *L*, use:

$$L = L_b(p) - G_t - G_r \quad \text{dB} \tag{72}$$

For clear-air interference scenarios where radio propagation is dominated by troposcatter, the elevation angles will be slightly greater than the radio horizon angles, θ_t and θ_r. The use of these should introduce negligible error, unless these also coincide with their respective stations' boresight directions.

5 Hydrometeor-scatter interference prediction

At frequencies above about 5 GHz, where the dimensions of hydrometeors are comparable to or greater than wavelengths, interference due to hydrometeor-scatter may have pronounced interactions. In contrast to the clear-air prediction methods described above, the hydrometeor-scatter interference prediction methodology described below develops expressions for the transmission loss between two stations directly, since it requires knowledge of the interfering and victim antenna radiation patterns for each station.

The method is quite general, and can be used with any antenna radiation pattern which provides a method for determining the antenna gain at any off-boresight angle. Radiation patterns such as those in Recommendations ITU-R F.699, ITU-R F.1245, ITU-R S.465 and ITU-R S.580, for example, can all be used, as can more complex patterns based on Bessel functions and actual measured patterns if these are available. The method can also be used with omnidirectional or sectorial antennas, such as those characterized in Recommendation ITU-R F.1336, the gain of which is generally determined from the vertical off-boresight angle (i.e. the elevation relative to the angle of maximum gain).

The method is also general in that it is not restricted to any particular geometry, provided that antenna radiation patterns are available. Thus, it includes both main beam-to-main beam coupling and side lobe-to-main beam coupling, and both great-circle scatter and side-scatter geometries. The

method can compute interference levels for both long-path (> 100 km) and short-path geometries (down to a few kilometres) with arbitrary elevation and azimuthal angles at either station. The methodology is therefore appropriate to a wide range of scenarios and services, including the determination of rain-scatter interference between two terrestrial stations, between a terrestrial station and an earth station, and between two earth stations operating in bi-directionally allocated frequency bands. The methodology is based on mathematical formulation describing the transmission loss due to hydrometeor scatter between two stations. The transmission loss formulation accounts only for single scattering from raindrops. Multiple scattering is neglected because of higher attenuation values attributed to both atmospheric gases and precipitation. Moreover, the hydrometeor scatter can be ignored for the following conditions:

– no precipitation between the two stations;

– frequency below 5 GHz;

the channel bandwidths of the two stations do not overlap, as the mechanism is unlikely to cause adjacent channel interference;

– the main beams of the station antennas are parallel to each other (78); and

– the off-axis squint angle of one station (79) is larger than its beamwidth.

The methodology developed below calculates hydrometeor scatter loss for a single case of main beam to main beam coupling. However, it can be adapted to calculate hydrometeor scatter loss due to either main beam to side lobe coupling or side lobe to main beam coupling. This can be achieved through substituting the characteristics of the main beam of the required station antenna with the characteristics of the side lobe. In this case all the parameters of the side lobe replace the corresponding parameters of the replaced main beam. For instance in replacing a main beam by side lobe, the scattering angle (78) and the squint angles (79) are measured with respect to the boresight of the used side lobe.

FIGURE 3

Flow chart of hydrometeor scatter algorithm

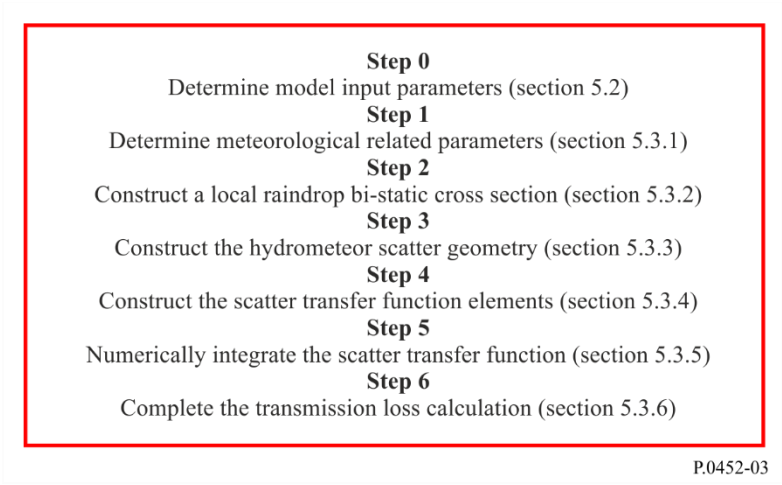

5.1 Theoretical basis of transmission loss due to hydrometeor scatter

The transmission loss, (dB), due to hydrometeor scattering between two stations, Station 1 with polarization q $(q = v, h)$and Station 2 with polarization p $(p = v, h)$, based on the bi-static radar equation is

$$L_{pq} = 73.4399 + 20 \log_{10} f - 10 \log_{10} C_{pq} \quad \text{dB} \tag{73}$$

where:

f: frequency (GHz)

C_{pq}: scatter transfer function including integration over rain cell volume ($m^{-1}km^{-1}$)

$$C_{pq} = \iiint \frac{G_1 G_2 \sigma_{pq}}{r_{A1}^2 r_{A2}^2} \exp(-c[\mathcal{K}_{atm} + \mathcal{K}_{rain}])\zeta(h)dV \quad (74)$$

NOTE – A numerical expression for this integral is provided in the remainder of this Annex as equations (132) and (133).

$G_{1,2}$: linear gains of Station 1 and Station 2, respectively

$r_{A1,2}$: distances from the integration element dV to Station 1 and Station 2 (km)

σ_{pq}: raindrop bi-static cross section per unit volume § 5.3.4.4 (m^2m^{-3})

c : $(c = 0.23026)$ constant to convert attenuation in dB to Nepers

$\mathcal{K}_{atm}$: attenuation due to atmospheric gases along the path from transmitter to receiver (dB) passing through the integration element; § 5.3.4.2

$\mathcal{K}_{rain}$: attenuation due to rain along the path from transmitter to receiver (dB) passing through the integration element; § 5.3.4.3

$\zeta(h)$: height dependence of the radar reflectivity:

$$\zeta(h) = \begin{cases} 1 & \text{for } h \le h_R \\ 10^{-0.65(h-h_R)} & \text{for } h > h_R \end{cases} \quad (75)$$

h_R: rain height (km);

dV: volume of differential integration element (km^3).

5.2 The model input parameters

TABLE 5

List of input parameters
(Suffix 1 refers to parameters for Station 1, suffix 2 refers to parameters for Station 2)

Parameter	Units	Description
d	km	Great-circle path distance
f	GHz	Frequency
h_{1_loc}, h_{2_loc}	km	Local heights above mean sea level of Station 1, Station 2
G_1, G_2	dB	Gain for each antenna as a function of both antenna boresight angle and antenna polarization
BW_1, BW_2	rad	Antenna beam widths. The beam widths could be for either main beams or side lobes depending on the required coupling.
$p_R(R)$		Probability distribution of rainfall rate
M	dB	Polarization mismatch between systems
P	hPa	Surface pressure (default 1 013.25 hPa)
$p_h(h)$		Probability distribution of rain height
T	°C	Surface temperature (default 15° C)
α_{1_loc}, α_{2_loc}	rad	Local bearings of Station 1 from Station 2, and Station 2 from Station 1, in the clockwise sense
ε_{H1_loc}, ε_{H2_loc}	rad	Local horizon angles for Station 1 and Station 2

TABLE 5 (*end*)

Parameter	Units	Description
ρ	g/m^3	Surface water-vapour density (default 8 g/m^3)
τ	degrees	Polarization angle of link (0° for horizontal polarization, 90° for vertical polarization)
Lat_1,2 Lon_1,2	degrees	Latitude and Longitude for Station 1 and Station 2
R_p		percentage subject quantity will not be exceeded

5.2.1 Link geometric parameters

Besides the above input parameters the link geometric parameters can be considered as input parameters. If not provided, these parameters are calculated and saved for future use.

FIGURE 4

Geometry of stations on curved Earth

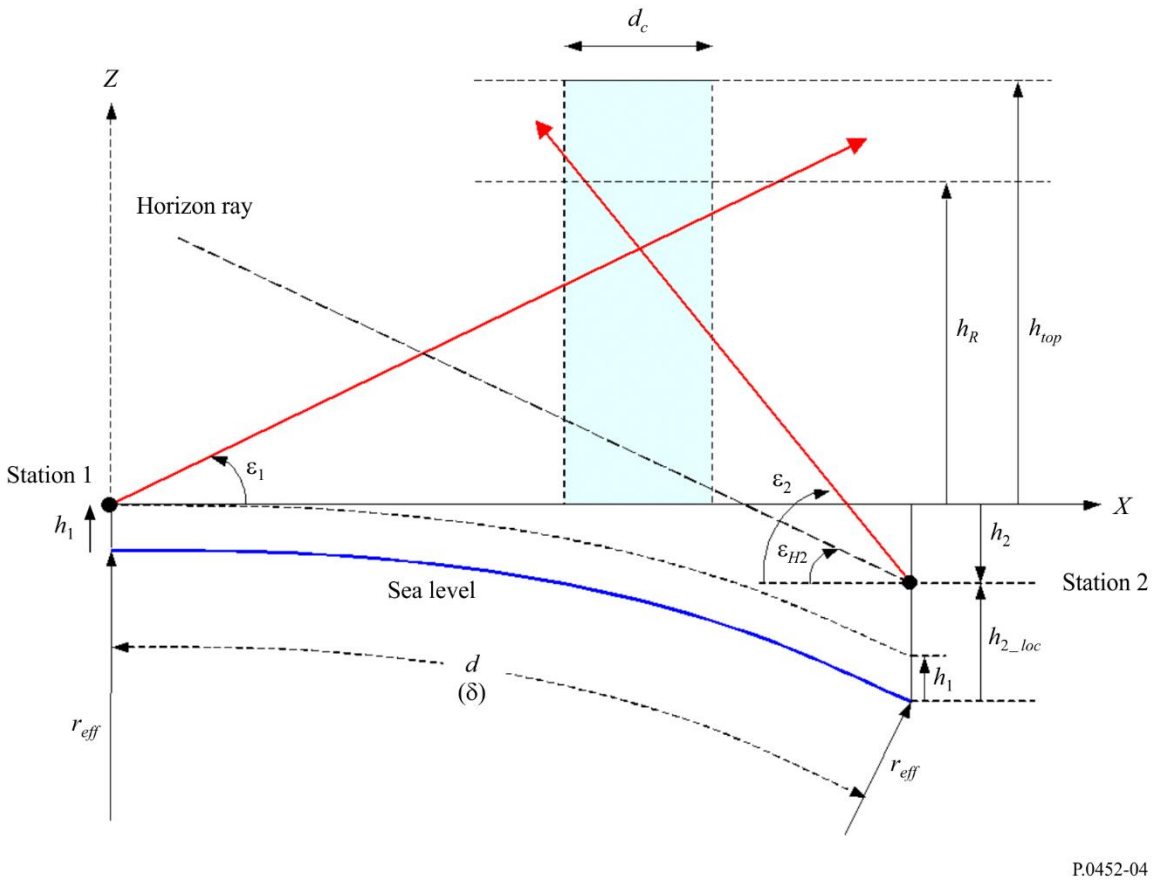

5.2.1.1 Station antenna boresight axes (main beams)

Figure 5 depicts the geometric configuration of the hydrometeor scatter link using the Cartesian coordinate of Station 1 as a common coordinate. In this coordinate, Station 1 is located at the origin $(0, 0, 0)$ with the x-y plane is the horizontal plane, the x-axis is pointing toward Station 2, and the z-axis is pointing vertically upward. The boresight axis of Station 1 antenna is given by the unit vector $\boldsymbol{V_{10}}$:

$$\boldsymbol{V_{10}} = \begin{bmatrix} \cos\varepsilon_1 \cos\alpha_1 \\ \cos\varepsilon_1 \sin\alpha_1 \\ \sin\varepsilon_1 \end{bmatrix} = \begin{bmatrix} x_{10} \\ y_{10} \\ z_{10} \end{bmatrix} \quad (76)$$

In equation (76), $\varepsilon_1 = \varepsilon_{1\_loc}$, and $\alpha_1 = \alpha_{1\_loc}$ with ε_{1_loc} and α_{1_loc} are the local elevation and azimuth angles of boresight axis of Station 1 antenna.

FIGURE 5

Schematic of hydrometeor scatter link geometry for the general case of side scattering

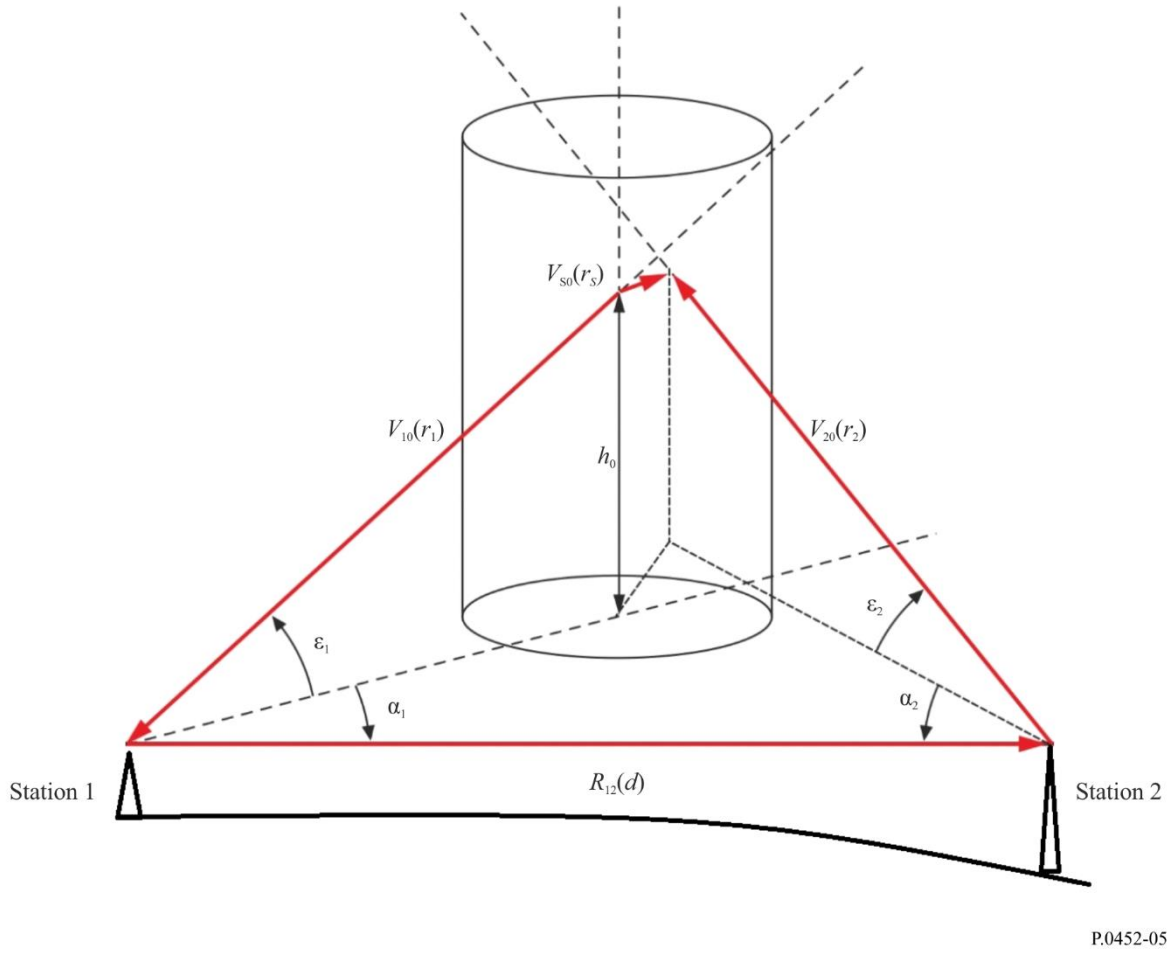

The boresight axis of Station 2 antenna is represented by unit-length vector $\mathbf{V_{20}}$:

$$\boldsymbol{V_{20}} = \begin{bmatrix} \cos\varepsilon_2 \cos\alpha_2 \\ \cos\varepsilon_2 \sin\alpha_2 \\ \sin\varepsilon_2 \end{bmatrix} = \begin{bmatrix} \sin\varepsilon_{2\_loc} \sin\delta - \cos\varepsilon_{2\_loc} \cos\alpha_{2\_loc} \cos\delta \\ -\cos\varepsilon_{2\_loc} \sin\alpha_{2\_loc} \\ \sin\varepsilon_{2\_loc} \cos\delta + \cos\varepsilon_{2\_loc} \cos\alpha_{2\_loc} \sin\delta \end{bmatrix} = \begin{bmatrix} x_{20} \\ y_{20} \\ z_{20} \end{bmatrix} \quad (77a)$$

The angles ε_2 and α_2 are the elevation and the azimuth angles of Station 2 from Station 1 in the common frame; and ε_{2_loc}, and α_{2_loc} are the corresponding angles in the local frame of Station 2 antenna. In addition, δ is the angle subtended by the two stations at the Earth centre ($\delta = d/r_{eff}$, $r_{eff} = a_e = k_{50}a$ is the effective (median) Earth radius, a is the average Earth radius, a (as determined in equation (6a)), and k_{50} (as determined in equation (5)) is the median radius factor). At small values of δ the Earth curvature could be ignored; and ε_2 and α_2 are equal to ε_{2_loc} and $\alpha_{2\_loc} + \pi$ respectively.

The vector from Station 1 to Station 2 is:

$$\boldsymbol{V_{12}} = \begin{bmatrix} 1 \\ 0 \\ 0 \end{bmatrix} \quad \text{and} \quad \boldsymbol{R_{12}} = \boldsymbol{V_{12}} \tag{77b}$$

5.2.1.2 The main beam scattering angle

The main beam scattering angle φ_{ms}, is the angle between the two antenna main beams (boresight axes) and it is determined from the scalar product of the two unit vectors $\mathbf{V_{10}}$ and $\mathbf{V_{20}}$:

$$\varphi_{ms} = \cos^{-1}(-\boldsymbol{V_{20}}.\boldsymbol{V_{10}}) = \cos^{-1}(-\{\cos\varepsilon_1 \cos\varepsilon_2 \cos(\alpha_1 - \alpha_2) + \sin\varepsilon_1 \sin\varepsilon_2\}) \tag{78}$$

If $\varphi_{ms} < 0.001$ rad, the two antenna beams are either approximately parallel or co-linear. If the antenna beams are approximately parallel to each other, coupling by rain scatter is negligible and there is no need to calculate hydrometeor scatter.

5.2.1.3 The off-axis squint angles

The off-axis squint angles $\psi_{1,2}$ at Station 1 or 2 of the point of closest approach on the other station main beam axis are given by

$$\Psi_{1,2} = \tan^{-1}\left(\frac{r_S}{r_{1,2}}\right) \tag{79}$$

The distances r_1, r_2 and r_s can be obtained from equation (80), where (x_{10}, y_{10}, z_{10}) and (x_{20}, y_{20}, z_{20}) are the components of the unit vectors $\boldsymbol{V_{10}}$ and $\boldsymbol{V_{20}}$ respectively.

$$\begin{bmatrix} r_s \\ r_1 \\ r_2 \end{bmatrix} = \begin{bmatrix} x_{S0} & x_{10} & -x_{20} \\ y_{S0} & y_{10} & -y_{20} \\ z_{S0} & z_{10} & -z_{20} \end{bmatrix}^{-1} \begin{bmatrix} d \\ 0 \\ h_2 \end{bmatrix}, \qquad h_2 = h_{2\_loc} - h_{1\_loc} - d\frac{\delta}{2} \text{ km} \tag{80}$$

In (80), h_2 is the height of Station 2 above the reference plane.

The operator $[\ ]^{-1}$ is the inverse matrix operator. As for x_{S0}, y_{S0}, and z_{S0}, they are components of the unit vector $\boldsymbol{V_{S0}}$ stemming from vector product of the unit vectors $\boldsymbol{V_{10}}$ and $\boldsymbol{V_{20}}$.

$$V_{S0} = \frac{\boldsymbol{V_{20}} \times \boldsymbol{V_{10}}}{\sin\varphi_{ms}} = \frac{1}{\sin\varphi_{ms}} \begin{bmatrix} y_{20}z_{10} - z_{20}y_{10} \\ z_{20}x_{10} - x_{20}z_{10} \\ x_{20}y_{10} - y_{20}x_{10} \end{bmatrix} = \begin{bmatrix} x_{S0} \\ y_{S0} \\ z_{S0} \end{bmatrix} \tag{81}$$

If a squint angle is less than the 3 dB beamwidth of the relevant antenna, main beam-to-main beam coupling is possible and calculating hydrometeor scatter is required.

5.3 Steps of applying the hydrometeor scatter algorithm

If it is determined that calculating transmission loss due to hydrometeor scatter is required, the following algorithm steps can be followed for getting the transmission loss.

5.3.1 Step 1: Determining meteorological related parameters

The meteorological related parameters required by the algorithm are:

– The atmospheric specific attenuation;

– The specific rain attenuation;

– Rain cell structure; and

– Rain height.

Here are the prescriptions for each parameter.

5.3.1.1 The atmospheric specific attenuation γ_{atm}

The atmospheric specific attenuation γ_{atm} is required for getting the attenuation due to atmospheric gases $\mathcal{K}_{atm}$ along the propagation path from the transmitter to the receiver passing through the scattering volume (see § 5.3.3). The atmospheric specific attenuation can be obtained from Annex 1 of Recommendation ITU-R P.676 in terms of the atmospheric temperature, pressure and water vapour density profile.

5.3.1.2 The specific rain attenuation γ_R

The rain specific attenuation prediction model in this Recommendation is different from that in Recommendation ITU-R P.838 and should only be used for the purposes as required in § 5 for hydrometeor-scatter interference prediction. The reason for this warning is because the rain specific attenuation prediction model of Recommendation ITU-R P.838 is developed for oblate spheroidal raindrops, while the hydrometeor scatter model is developed for spherical raindrops. This difference has an impact on formulations that include the specific rain attenuation formulations of equations (82) to (87), the raindrop bistatic cross section formulations of equations (123a) to (123d). Furthermore, the rain specific attenuation model of Recommendation ITU-R P.838 has no temperature dependence, while both the rain specific attenuation and the bistatic cross section in this section have temperature dependence.

The specific rain attenuation γ_R is required for calculating attenuation due to rain $\mathcal{K}_{rain}$ along the propagation path from the transmitter to the receiver passing through the scattering volume and it is given in terms of rainfall rate R by:

$$\gamma_{R1,2} = \kappa_{1,2} R^{\alpha_{1,2}} \quad \text{(dB/km)} \tag{82}$$

The coefficients $\kappa_{1,2}$ and $\alpha_{1,2}$ are functions of frequency f (GHz), and raindrop temperature as given in equations (83) to (85).

$$\alpha_{1,2} = a_0 + a_1 x + a_2 x^2 + a_3 x^3 + a_4 x^4 + a_5 x^5 + a_6 x^6 \tag{83}$$

$$\kappa_{1,2} = \exp(b_0 + b_1 x + b_2 x^2 + b_3 x^3 + b_4 x^4 + b_5 x^5) \tag{84}$$

$$x = \ln(f) \tag{85}$$

The coefficients a_m of equation (83) and the coefficients b_n of equation (84) depend on the temperature T (°C).

The dependence on temperature of each of the coefficients a_n and b_n can be written as:

$$a_m = c_0^m + c_1^m T + c_2^m T^2, \quad m = 0,1,2,3,4,5,6 \tag{86}$$

$$b_m = d_0^m + d_1^m T + d_2^m T^2, \quad m = 0,1,2,3,4,5 \tag{87}$$

Tables 6 and 7 provide values of c_i^m and d_i^m ($i = 0,1,2$).

5.3.1.3 The rain cell structure

The rain cell has a cylindrical symmetry within the horizontal cross-section, where the rainfall rate is assumed to decay exponentially away from the rain cell centre, and it can be expressed as:

$$R(\rho) = R_m \exp(-\rho/\rho_0) \quad \text{mm/hr} \tag{88}$$

where ρ is the radial distance from the centre of the rain cell, R_m is the peak rain rate at the centre, and ρ_0 is a "characteristic distance" from the cell centre with:

$$\rho_0 = \frac{10 - 1.5 \log_{10} R_m}{\ln\left(\frac{R_m}{0.4}\right)} \quad \text{km}, \quad R_m > 0.4 \text{ mm/hr} \tag{89}$$

5.3.1.4 Rain height

The mean annual rain height above mean sea level, h_R, which is in the range of 4 to 5 km, can be obtained from the 0 °C isotherm height h_{iso}.

$$h_R = h_{iso} + 0.36 \quad \text{km} \tag{90}$$

The mean annual 0 °C isotherm height above mean sea level, h_{iso} can be calculated using Recommendation ITU-R P.839-4 R-REC-P.839-4-201309-I!!ZIP-E

5.3.2 Step 2: Constructing a local raindrop bi-static cross section

The raindrop bi-static cross section η_1 in the local frame of the symmetric raindrop can be written in terms of the scattering angle φ_s as follows.

$$\eta_1(\varphi) = \exp\{u_0 + u_1(\sin 0.5\varphi_s)^2 + u_2(\sin 0.5\varphi_s)^4 + u_3(\sin 0.5\varphi_s)^6\} \tag{91}$$

The coefficients $u_i's$ $(i = 0,1,2,3)$ in equation (91) are related to rainfall rate as in equation (92)

$$\begin{aligned} u_i &= a_0^i + a_1^i \ln(R) + a_2^i \{\ln(R)\}^2, \qquad i = 0,1 \\ u_i &= a_0^i + a_1^i \ln(R) + a_2^i \{\ln(R)\}^2 + a_3^i \{\ln(R)\}^3, \quad i = 2,3 \end{aligned} \tag{92}$$

Furthermore, the dependence of each of the coefficients $a_n^i's$ of equation (92) on the frequency f can be captured into an algebraic polynomial of sixth order.

$$a_n^i = \sum_{m=0}^{7} b_{n,m}^i f^m \ , \quad i = 0,1,2,3 \ and \ n = 0,1,2,3 \tag{93}$$

Moreover, each of the coefficients $b_{n,m}^i's$ of equation (93) is related to the temperature T as in equation (94).

$$b_{n,m}^i = c_0 + c_1 T + c_2 T^2 \tag{94}$$

Values of the coefficients $c_0's$, $c_1's$ and $c_2's$ are provided in Tables 8 to 21.

5.3.3 Step 3: Constructing hydrometeor scatter geometry

The hydrometeor scatter geometry is constructed (using flat-Earth approximation) by constructing a rain cell with its vertical axis intersecting the main beam axis of Station 1 at point 0 (x_0, y_0, h_0) as shown in Fig. 6.

$$\begin{aligned} x_0 &= r_1 \cos\varepsilon_1 \cos\alpha_1 \\ y_0 &= r_1 \cos\varepsilon_1 \sin\alpha_1 \\ h_0 &= r_1 \sin\varepsilon_1 \end{aligned} \tag{95}$$

The distance r_1 in equation (95) can be obtained from equation (80). In constructing the hydrometeor scatter geometry, the centre of the rain cell may be varied depending on the scenarios that minimize values of transmission losses, and hence maximize the interfering scattered power. A point A (*x*, *y*, *h*) within the cell represents an arbitrary integration element and a point B is the projection of the point A on the ground plane (see Fig. 6).

FIGURE 6

Hydrometeor scatter geometry

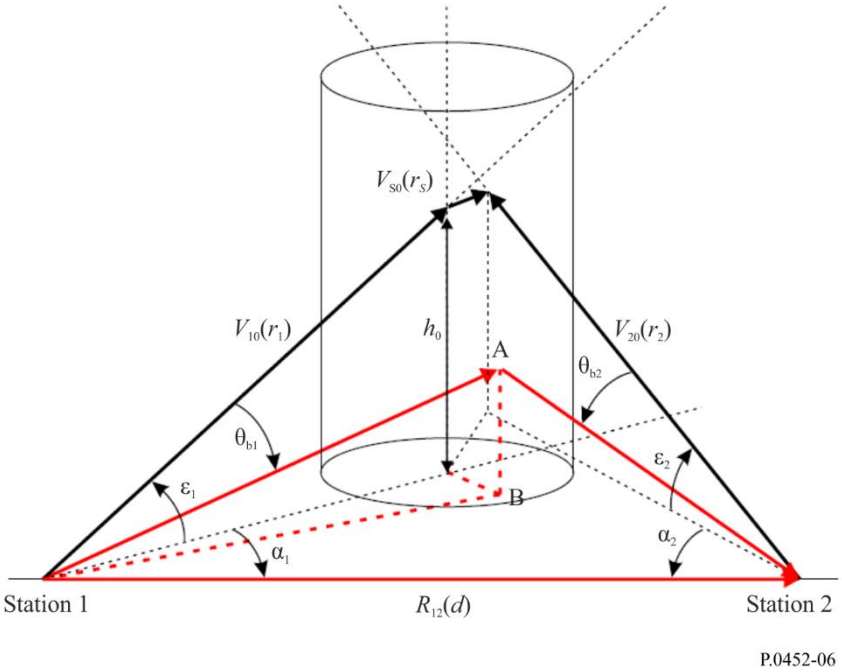

To facilitate carrying out the integration of the scatter transfer function of equation (74), the Cartesian coordinate of the integration element A (x, y, h) is converted into a cylindrical coordinate (ρ, φ, z).

$$x = x_0 + \rho \cos\varphi$$
$$y = y_0 + \rho \sin\varphi$$
$$h = h_0 + z$$
$$dV = \rho \, d\rho d\varphi dz \tag{96}$$

The centre of the cylindrical coordinate is the point 0 (x_0, y_0, h_0) where the rain cell vertical axis intersects with Station 1 boresight axis. Within the cylindrical coordinates, the distances $r_{A1,2}$ from Station 1 and Station 2 to the integration element at A (ρ, φ, z) can be expressed as follows:

$$r_{A1} = r_1' D_{A1}, \quad D_{A1} = \sqrt{1 + \{\rho^2 + z^2 + 2\rho d_1' \cos(\alpha_1 - \varphi) + 2h_0 z\}/(r_1')^2}$$
$$r_1' = \sqrt{(d_1')^2 + h_0^2}, \qquad d_1' = \sqrt{x_0^2 + y_0^2}$$
$$\alpha_1 = \tan^{-1}\left(\frac{y_0}{x_0}\right)$$
$$r_{A2} = r_2' D_{A2}$$
$$D_{A2} = \sqrt{1 + \{\rho^2 + z^2 + 2\rho d_2' \cos(\alpha_2 - \varphi) + 2(h_0 - h_2) z\}/(r_2')^2} \tag{97}$$
$$r_2' = \sqrt{(d_2')^2 + (h_0 - h_2)^2}, \quad d_2' = \sqrt{(x_0 - d)^2 + y_0^2}$$
$$\alpha_2 = \tan^{-1}\left(\frac{y_0}{x_0 - d}\right)$$

The position vectors $\boldsymbol{R_{A1,2}}(\rho, \varphi, z)$ are given by

$$\boldsymbol{R_{A1}}(\rho,\varphi,z)=\begin{bmatrix}\mathrm{x}\\ \mathrm{y}\\ h\end{bmatrix}=\begin{bmatrix}x_0+\rho\cos\varphi\\ y_0+\rho\sin\varphi\\ h_0+z\end{bmatrix}=r_{A1}\begin{bmatrix}\cos\varepsilon_{A1}\cos\alpha_{A1}\\ \cos\varepsilon_{A1}\sin\alpha_{A1}\\ \sin\varepsilon_{A1}\end{bmatrix} \tag{98a}$$

$$\boldsymbol{R_{A2}}(\rho,\varphi,z)=\begin{bmatrix}\mathrm{x}-\mathrm{d}\\ \mathrm{y}\\ h-h_2\end{bmatrix}=\begin{bmatrix}x_0+\rho\cos\varphi-d\\ y_0+\rho\sin\varphi\\ h_0+z-h_2\end{bmatrix}=r_{A2}\begin{bmatrix}\cos\varepsilon_{A2}\cos\alpha_{A2}\\ \cos\varepsilon_{A2}\sin\alpha_{A2}\\ \sin\varepsilon_{A2}\end{bmatrix} \tag{98b}$$

with

$$|\boldsymbol{R_{A1}}|=\sqrt{(x_0+\rho\cos\varphi)^2+(y_0+\rho\sin\varphi)^2+(h_0+z)^2}=r_{A1} \tag{99a}$$

and

$$|\boldsymbol{R_{A2}}|=\sqrt{(x_0+\rho\cos\varphi-d)^2+(y_0+\rho\sin\varphi)^2+(h_0+z-h_2)^2}=r_{A2} \tag{99b}$$

Furthermore, the elevation angles $\varepsilon_{A1,2}$ of the position vectors $\boldsymbol{R_{A1,2}}(\rho,\varphi,z)$ are given by

$$\varepsilon_{A1}=\tan^{-1}\left(\frac{h_0+z}{d_{B1}}\right) \tag{100a}$$

$$\varepsilon_{A2}=\tan^{-1}\left(\frac{(h_0-h_2)+z}{d_{B2}}\right) \tag{100b}$$

where:

$$d_{B1}=\sqrt{x^2+y^2}=\sqrt{d'^2_1+\rho^2+2\rho d'_1\cos(\alpha_1-\varphi)}$$

and

$$d_{B2}=\sqrt{(x-d)^2+y^2}=\sqrt{(d'_2)^2+\rho^2+2\rho d'_2\cos(\alpha_2-\varphi)} \tag{101}$$

It should be noted that $r_{A1}=\sqrt{(d_{B1})^2+(h_0+z)^2}$, and $r_{A2}=\sqrt{(d_{B2})^2+(h_0-h_2+z)^2}$. Moreover, in getting (100a), and (100b) the far right side of equations (98a) and (98b) are used respectively along with equation (101)

The azimuth angles $\alpha_{A1,2}$ of the position vectors $\boldsymbol{R_{A1,2}}(\rho,\varphi,z)$ are:

$$\begin{aligned}\alpha_{A1}&=\tan^{-1}\left(\frac{y_0+\rho\sin\varphi}{x_0+\rho\cos\varphi}\right)\\ \alpha_{A2}&=\tan^{-1}\left(\frac{y_0+\rho\sin\varphi}{x_0-d+\rho\cos\varphi}\right)\end{aligned} \tag{102}$$

Based on equation (96), the integral of the scatter transfer function in equation (74) can be reduced into:

$$C_{pq}=\int_{z_{min}}^{z_{max}}\int_0^{2\pi}\int_0^{\rho_{max}}\mathcal{F}(\rho,\varphi,z)\,\rho d\rho d\varphi dz \tag{103}$$

$$\mathcal{F}(\rho,\varphi,z)=\frac{G_1(\theta_{A1})G_2(\theta_{A2})\sigma_{pq}\exp\left(-c\mathcal{K}(A)\right)\zeta(h)}{r_{A1}^2r_{A2}^2} \tag{104}$$

$\mathcal{K}(A)$ is the attenuation from Station 1 to Station 2 passing through the point A with

$$\mathcal{K}(A)=\mathcal{K}_{atm}(A)+\mathcal{K}_{rain}(A) \tag{105}$$

In equation (105), $\mathcal{K}_{atm}(A)$ and $\mathcal{K}_{rain}(A)$ are the attenuation from Station 1 to Station 2 passing through the point *A* due to atmospheric gases and rain respectively.

For the integration limits in equation (103), the minimum and maximum heights, z_{min} and z_{max} are determined by the beam widths of Station 1 and Station 2.

$$z_{1max} = \sqrt{x_0^2 + y_0^2}\tan(\epsilon_1 + 0.5BW_1) - h_0 \quad (106)$$

$$z_{1min} = \sqrt{x_0^2 + y_0^2}\tan(\epsilon_1 - 0.5BW_1) - h_0 \quad (107)$$

$$z_{2max} = \sqrt{(x_0 - d)^2 + y_0^2}\tan(\epsilon_2 + 0.5BW_2) - h_0 \quad (108)$$

$$z_{2min} = \sqrt{(x_0 - d)^2 + y_0^2}\tan(\epsilon_2 - 0.5BW_2) - h_0 \quad (109)$$

$$z_{max} = \min\{\max(z_{1max}, z_{2max}), h_R\} \quad (110)$$

$$z_{min} = \min(z_{1min}, z_{2min}) \quad (111)$$

BW_1 and BW_2 are beam width of Station 1 and Station 2 respectively given in radian values. As for ρ_{max} determining the integration limit over $d\rho$ it is given by equation (112).

$$\rho_{max} = \frac{1}{2}\{\rho_1 + \rho_2\} \quad \text{km} \quad (112)$$

$$\rho_1 = x_0 - \frac{d}{1 + \tan(\varepsilon_1 + 0.5BW_1)\cot(\varepsilon_2 - 0.5BW_2)} \quad \text{km} \quad (113)$$

$$\rho_2 = (d - x_0) - \frac{d}{1 + \tan(\varepsilon_2 + 0.5BW_2)\cot(\varepsilon_1 - 0.5BW_1)} \quad \text{km} \quad (114)$$

The near field intensities of antennas are dependent on specific hardware details which may not be available in undertaking interference analysis. It is appropriate to assume that the field strength will be approximately the same order of magnitude as at the beginning of the far-field region. This approximation agrees with actual measurements of near field intensities.

The scattering angle φ_s from Station 1 to the integration point A is:

$$\varphi_s = \cos^{-1}\left(-\frac{r_{A1}}{r_{A2}} + \frac{d(x_0 + \rho\cos\varphi) + h_2(h_0 + z)}{r_{A1}r_{A2}}\right) \quad (115)$$

5.3.4 Step 4: Constructing the scattering transfer function elements

5.3.4.1 Antenna gains

Antenna gains G_1 and G_2 at the integration element $A(\rho, \varphi, z)$ can be obtained through introducing values off boresight angles $\theta_{A1,2}$ into the corresponding gain pattern provided within the input parameters of Table 6. The off boresight angle θ_{A1} is the angle between the unit vector V_{A1}extending from Station 1 to the integration element, and the main beam direction of Station 1. This angle is given by:

$$\theta_{A1} = \cos^{-1}\{\cos\varepsilon_1\cos\varepsilon_{A1}\cos(\alpha_1 - \alpha_{A1}) + \sin\varepsilon_1\sin\varepsilon_{A1}\} \quad (116)$$

The off boresight angle θ_{A2} is the angle between the unit vector V_{A2} extending from Station 2 to the integration element, and the main beam of Station 2. This angle is given by:

$$\theta_{A2} = \cos^{-1}\{\cos\varepsilon_2\cos\varepsilon_{A2}\cos(\alpha_2 - \alpha_{A2}) + \sin\varepsilon_2\sin\varepsilon_{A2}\} \quad (117)$$

5.3.4.2 Atmospheric attenuation

The attenuation $\mathcal{K}_{atm}$ due to absorption by atmospheric gases along the propagation paths to the integration element located at the point $A(\rho, \varphi, z)$ can be calculated from the atmospheric specific attenuation γ_{atm} provided in § 5.3.1.1.

Dividing the propagation distances $r_{A1,2}$ into $N_{1,2}$ intervals of lengths $\Delta h_{t1,2}/\sin\varepsilon_{A1,2}$ leads to the following summations, intervals are defined in § 5.3.4.3.

$$\mathcal{K}_{atm} = \sum_{t1=1}^{N_1} \frac{\gamma_{atm}(t1)\Delta h_{t1}}{\sin \epsilon_{A1}} + \sum_{t2=1}^{N_2} \frac{\gamma_{atm}(t2)\Delta h_{t2}}{\sin \epsilon_{A2}} \approx \sum_{t1=1}^{N_1} \frac{\gamma_{atm}(t1) r_{A1}}{\mathrm{N}_1} + \sum_{t2=1}^{N_2} \frac{\gamma_{atm}(t2) r_{A2}}{\mathrm{N}_2} \quad (118)$$

5.3.4.3 Attenuation due to rain

Similar to the attenuation due to atmospheric gases, the attenuation $\mathcal{K}_{rain}$ along the propagation paths to the integration element located at the point $A(\rho, \varphi, z)$ can be calculated from the rain specific attenuation $\gamma_{R1,2}$ provided in § 5.3.1.2.

Dividing the propagation distances $r_{A1,2}$ into $N_{1,2}$ intervals of lengths $\Delta h_{t1,2}/\sin \varepsilon_{A1,2}$ leads to the following summations.

$$\mathcal{K}_{rain} = \sum_{t1=1}^{N_1} \frac{\gamma_{R1}(t1)\Delta h_{t1}}{\sin \epsilon_{A1}} + \sum_{t2=1}^{N_2} \frac{\gamma_{R2}(t2)\Delta h_{t2}}{\sin \epsilon_{A2}} \quad (119)$$

First parametrize the propagation path with parameter *t* on interval (0,1) from point (0,0,0) to integration point A as follows:

$$s(t) = \boldsymbol{R_{A1}} t + (0,0,0) = \begin{bmatrix} x_0 + \rho \cos \varphi \\ y_0 + \rho \sin \varphi \\ h_0 + z \end{bmatrix} t \quad (120)$$

$$|\boldsymbol{R_{A1}}| = \sqrt{x^2 + y^2 + z^2} = \sqrt{(x_0 + \rho \cos \varphi)^2 + (y_0 + \rho \sin \varphi)^2 + (h_0 + z)^2} \quad (121)$$

So for N_1 integration points the factor $\frac{\Delta h_{t1}}{\sin \varepsilon_{A1}} = \frac{r_{A1}}{N_1}$

Second parametrize the propagation path with parameter *t* on interval (0,1) from point $(d, d \sin \alpha_1, h_{2\_\mathrm{loc}})$ to integration point A as follows:

$$s(t) = \boldsymbol{R_{A2}} t + \begin{bmatrix} d \\ d \sin \alpha_1 \\ h_{2\_\mathrm{loc}} \end{bmatrix} = \begin{bmatrix} x_0 + \rho \cos \varphi - d \\ y_0 + \rho \sin \varphi + d \sin \alpha_1 \\ h_0 + z - h_2 \end{bmatrix} t + \begin{bmatrix} d \\ d \sin \alpha_1 \\ h_2 \end{bmatrix} \quad (122)$$

So for N_2 integration points the factor $\frac{\Delta h_{t2}}{\sin \varepsilon_{A1}} = \frac{r_{A2}}{N_2}$.

5.3.4.4 Bi-static cross section in the common frame

At the integration element $A(\rho, \varphi, z)$, the raindrop local bi-static cross sections η_1 of equation (91) can be used to formulate the bi-static cross sections in the common frame σ_{pq}'s.

$$\sigma_{vv} = \eta_1 \{\cos \varphi_s \cos \alpha_{vs} \cos \alpha_{vi} + \sin \alpha_{vs} \sin \alpha_{vi}\}^2 \quad (123a)$$

$$\sigma_{vh} = \eta_1 \{\cos \varphi_s \cos \alpha_{vs} \sin \alpha_{vi} - \sin \alpha_{vs} \cos \alpha_{vi}\}^2 \quad (123b)$$

$$\sigma_{hv} = \eta_1 \{\cos \varphi_s \sin \alpha_{vs} \cos \alpha_{vi} - \cos \alpha_{vs} \sin \alpha_{vi}\}^2 \quad (123c)$$

$$\sigma_{hh} = \eta_1 \{\cos \varphi_s \sin \alpha_{vs} \sin \alpha_{vi} + \cos \alpha_{vs} \cos \alpha_{vi}\}^2 \quad (123d)$$

The angles α_{vi} and α_{vs} are the angles that rotate from the incident $\hat{v}_i$ and scattered $\hat{v}_s$ vertical polarizations anticlockwise to the polarization perpendicular to the scattering plane § 5.3.3. The scattering plane of raindrop is the plane formed by the incident and scattered directions.

The angle α_{vi} is given by

$$\alpha_{vi} = \tan^{-1} \left\{ \frac{(h_0+z)\left((x_0+\rho \cos \varphi)(x_0-d+\rho \cos \varphi) + (y_0+\rho \sin \varphi)^2\right) - d_{B1}^2 (h_0-h_2+z)}{r_{\mathrm{A1}} d (y_0+\rho \sin \varphi)} \right\} \quad (124)$$

The rotation angle α_{vs} is

$$\alpha_{vs} = \cos^{-1}\left\{ -\sin \alpha_{vi} \left(\hat{h}_{A1} . \hat{v}_{A2}\right) + \cos \alpha_{vi} \left(\hat{v}_{A1} . \hat{v}_{A2}\right) \right\} \quad (125)$$

with

$$\left(\hat{h}_{A1} \cdot \hat{v}_{A2}\right) = \frac{\{(h_0-h_2)+z\}(y_0+\rho\sin\varphi)}{d_{B1}d_{B2}r_{A2}}d \tag{126}$$

$$\left(\hat{h}_{A1} \cdot \hat{v}_{A2}\right) = \frac{1}{d_{B1}\sqrt{1+(h_0+z-h_2)^2}}\left(-(y_0+\rho\sin\varphi)+\frac{(x_0+\rho\cos\varphi)}{d_{B2}(h_0+z-h_2)}\right) \tag{127}$$

and

$$(\hat{v}_{A1} \cdot \hat{v}_{A2}) = \frac{d_{B1}^2 r_{A2}^2+\{(h_0-h_2)+z\}\{h_2 d_{B1}^2-(h_0+z)(x_0+\rho\cos\varphi)d\}}{r_{A1}d_{B1}r_{A2}d_{B2}} \tag{128}$$

$$(\hat{v}_{A1} \cdot \hat{v}_{A2}) = \frac{1}{1+(h_0+z-h_2)^2}\left(1+\frac{1}{d_{B1}^2(h_0+z-h_1)^2}+\frac{d_{B2}^2 r_2^2}{(h_0+z-h_2)^2}\right) \tag{129}$$

5.3.5 Step 5: Integration of the scatter transfer function

The integration of the scatter transfer function (equation (103)) can be performed using any suitable numerical integration technique such as the Legendre-Gauss quadrature technique applied below.

5.3.5.1 Integration by Legendre-Gauss quadrature

In applying the Legendre-Gauss quadrature, the following change of variables is used

$$\rho = \frac{\rho_{max}}{2}(\chi+1)$$

$$\varphi = \pi(\eta+1)$$

$$z = \frac{(z_{max}-z_{min})}{2}\varsigma + \frac{(z_{max}+z_{min})}{2} \tag{131}$$

with $-1 \le \chi, \eta, \varsigma \le 1$.

Introducing equation (131) into equations (103-104) and using Legendre-Gauss quadrature yields:

$$C_{pq} = \sum_{n=1}^{M_3} \mathcal{H}_n \tag{132}$$

$$\mathcal{H}_n = \frac{\pi(z_{max}-z_{min})d_c^2}{4} w_n \sum_{i=1}^{M_1} w_i \sum_{j=1}^{M_2} w_j \mathcal{F}_{ijn}(\chi_i, \eta_j, \varsigma_n) \tag{133}$$

Note: $\mathcal{F}_{ijn}(\chi_i, \eta_j, \varsigma_n) \rightarrow \mathcal{F}(\rho, \varphi, z)$ via equation (104).

M_1, M_2 and M_3 are the total numbers of integration points. Furthermore, χ_i $(i = 1, \ldots, M_1)$, η_j $(j = 1, \ldots, M_2)$, and ς_n $(n = 1, \ldots\ldots, M_3)$ are Gauss quadrature nodes; and w_i, w_j, and w_n are the corresponding weights from ITU-R P.1144.

The integration procedure using equations (131) to (133) is as follows:

1) Determine the Gauss quadrature points χ_i $(i = 1, \ldots, M_1)$ and η_j $(j = 1, \ldots, M_2)$; and the corresponding weights w_i and w_j from § 5.3.7.

2) Introduce the Gauss quadrature points into equation (131) to calculate the radii $\rho_i's$, the azimuth angles φ_j's and heights $z_n's$ within the integration volume.

3) Start with the lower layer within the rain cell $(n = 1)$ with the quadrature node $\varsigma_1$and weight w_1.

4) Use the resultant radii, azimuth angles, and height (ρ_i, φ_j, z_1) to calculate values of the parameters reported in equations (97) to (102).

5) For each point, use the above values to determine the off boresight angles (equations (116) and (117)) and hence the gain of each antenna, the bi-static cross sections, equations (123a) to (123d), the atmospheric attenuation (equation (118)), and rain attenuation (equation (119)).

6) Use the outcomes of procedure 5) in calculating the corresponding function $\mathcal{F}_{ij1}(\chi_i, \eta_j, \varsigma_1)$ given in equation (104).

7) Multiply each $\mathcal{F}_{ij1}(\chi_i, \eta_j, \varsigma_1)$ by the corresponding Gauss weights (w_i, w_j, and w_1).

8) Sum all values of $\mathcal{F}_{ij1}(\chi_i, \eta_j, \varsigma_1)$ and multiply the result by $\frac{\pi(z_{max}-z_{min})d_c^2}{4}$ yielding $\mathcal{H}_1$ as in equation (133) with $n = 1$.

9) Repeat procedures 1 through 8 with increasing the order of n by 1 ($n = 1, \dots, M_3$) to get values of all $\mathcal{H}_n$ ($n = 1, \dots, M_3$) as given in equation (133).

10) Sum all values of $\mathcal{H}_n$ ($n = 1, \dots, M_3$) and divide the resultant over $(r_1 r_2')^2$ to get the value of the scatter transfer function C_{pq} as given in equation (132).

5.3.6 Tables for section 5.3.1.2

TABLE 6

Values of the coefficients $c_i^m (i = 0, 1, 2)$ of equation (86)

m	c_0^m	c_1^m	c_2^m
0	0.86481	0.0025984	−3.2727e-05
1	−0.32507	−0.025593	0.00040852
2	0.70075	0.041632	−0.00084479
3	−0.4162	−0.023144	0.00063446
4	0.11971	0.0054147	−0.00022071
5	−0.018495	−0.00049312	3.6339e-05
6	0.0012143	8.1571e-06	−2.2949e-06

TABLE 7

Values of the coefficients d_i^m $(i = 0, 1, 2)$ of equation (87)

m	d_0	d_1	d_2
0	−9.2859	−0.026677	7.4162e-05
1	1.5977	−0.021172	0.001127
2	0.45627	−0.0010862	−0.0014558
3	−0.15347	0.016763	0.00066036
4	0.040141	−0.0062665	−0.00012758
5	−0.0049951	0.00064387	8.9007e-06

5.3.7 Tables for section 5.3.2

TABLE 8

Values of coefficients $c_0^{0,0,m}$, $c_1^{0,0,m}$ and $c_2^{0,0,m}$ for $b_{0,m}^0$ of equation (94) in case of a_0^0 of u_0 of equation (92)

m	c_0	c_1	c_2
0	−23.033	−0.019039	−1.3511e-07
1	1.0988	0.0057909	−1.8732e-05
2	−0.053826	−0.00051258	2.8893e-06
3	0.0017167	2.0326e-05	−1.5242e-07
4	−3.3231e-05	−4.2625e-07	3.8089e-09
5	3.7396e-07	4.9297e-09	−4.969e-11
6	−2.2438e-09	−2.9763e-11	3.2787e-13
7	5.5409e-12	7.3317e-14	−8.6497e-16

TABLE 9

Values of coefficients $c_0^{0,1,m}$, $c_1^{0,1,m}$ and $c_2^{0,1,m}$ for $b_{1,m}^0$ of equation (94) in case of a_1^0 of u_0 of equation (92)

m	$c_0^{0,1,m}$	$c_1^{0,1,m}$	$c_2^{0,1,m}$
0	1.758	0.0078061	−0.00019642
1	−0.034774	−0.0010409	4.8582e-05
2	0.0031934	1.2441e-05	−3.9051e-06
3	−0.00014758	1.6661e-06	1.5195e-07
4	3.3014e-06	−7.0142e-08	−3.2085e-09
5	−3.8772e-08	1.1439e-09	3.7652e-11
6	2.3188e-10	−8.5799e-12	−2.3101e-13
7	−5.5887e-13	2.4612e-14	5.779e-16

TABLE 10

Values of coefficients $c_0^{0,2,m}$, $c_1^{0,2,m}$ and $c_2^{0,2,m}$ for $b_{2,m}^0$ of equation (94) in case of a_2^0 of u_0 of equation (92)

m	$c_0^{0,2,m}$	$c_1^{0,2,m}$	$c_2^{0,2,m}$
0	−0.051224	0.00081531	1.1534e-05
1	0.0011587	−0.00031961	−2.3173e-06
2	−8.8754e-05	3.5484e-05	1.4933e-07
3	9.6328e-07	−1.6609e-06	−4.7112e-09
4	5.927e-08	3.9523e-08	8.0972e-11
5	−1.6618e-09	−5.0408e-10	−7.7464e-13
6	1.5626e-11	3.2862e-12	3.8749e-15
7	−5.0972e-14	−8.6057e-15	−7.8859e-18

TABLE 11

Values of coefficients $c_0^{1,0,m}$, $c_1^{1,0,m}$ and $c_2^{1,0,m}$ for $b_{0,m}^1$ of equation (94) in case of a_0^1 of u_1 of equation (92)

m	$c_0^{1,0,m}$	$c_1^{1,0,m}$	$c_2^{1,0,m}$
0	0.28927	0.037271	−0.00010078
1	−0.11742	−0.011059	6.6665e-05
2	0.010231	0.00093297	−8.6068e-06
3	−0.00041831	−3.5477e-05	4.2065e-07
4	8.8529e-06	7.2358e-07	−1.0192e-08
5	−1.0313e-07	−8.2014e-09	1.3111e-10
6	6.2591e-10	4.8736e-11	−8.5865e-13
7	−1.5469e-12	−1.1849e-13	2.2546e-15

TABLE 12

Values of coefficients $c_0^{1,1,m}$, $c_1^{1,1,m}$and $c_2^{1,1,m}$ for $b_{1,m}^1$ of equation (94) in case of a_1^1 of of u_1 of equation (92)

m	$c_0^{1,1,m}$	$c_1^{1,1,m}$	$c_2^{1,1,m}$
0	−0.2317	−0.005093	0.00045796
1	0.020016	−0.00076558	−0.00011298
2	0.00060157	0.00020785	9.1237e-06
3	−9.7303e-05	−1.2384e-05	−3.5392e-07
4	3.2711e-06	3.3064e-07	7.4324e-09
5	−5.0187e-08	−4.5084e-09	−8.6694e-11
6	3.6714e-10	3.0694e-11	5.2868e-13
7	−1.0386e-12	−8.2853e-14	−1.3148e-15

TABLE 13

Values of coefficients $c_0^{1,2,m}$, $c_1^{1,2,m}$and $c_2^{1,2,m}$ for $b_{2,m}^1$ of equation (94) in case of a_2^1 of u_1 of equation (92)

m	$c_0^{1,2,m}$	$c_1^{1,2,m}$	$c_2^{1,2,m}$
0	−0.036841	−0.0025519	−2.6162e-05
1	0.012953	0.00084793	5.2688e-06
2	−0.001305	−8.5265e-05	−3.3134e-07
3	5.9518e-05	3.7912e-06	9.6604e-09
4	−1.454e-06	−8.7204e-08	−1.4711e-10
5	1.91e-08	1.085e-09	1.1752e-12
6	−1.2719e-10	−6.9419e-12	−4.3973e-15
7	3.3748e-13	1.7914e-14	5.0804e-18

TABLE 14

Values of coefficients $c_0^{2,0,m}$, $c_1^{2,0,m}$ and $c_2^{2,0,m}$ for $b_{0,m}^2$ of equation (94) in case of a_0^2 of u_2 of equation (92)

m	$c_0^{2,0,m}$	$c_1^{2,0,m}$	$c_2^{2,0,m}$
0	−0.0022144	−0.0014792	0.00030493
1	−0.008123	−0.00055742	−8.8598e-05
2	0.0018507	0.00015755	8.3245e-06
3	−8.484e-05	−8.944e-06	−3.572e-07
4	1.9127e-06	2.323e-07	7.9876e-09
5	−2.2827e-08	−3.1221e-09	−9.6893e-11
6	1.4148e-10	2.1074e-11	6.0585e-13
7	−3.5797e-13	−5.6545e-14	−1.5317e-15

TABLE 15

Values of coefficients $c_0^{2,1,m}$, $c_1^{2,1,m}$ and $c_2^{2,1,m}$ for $b_{1,m}^2$ of equation (94) in case of a_1^2 of u_2 of equation (92)

m	$c_0^{2,1,m}$	$c_1^{2,1,m}$	$c_2^{2,1,m}$
0	−0.048207	−0.019603	3.8001e-06
1	−0.00041118	0.0045669	−1.0444e-05
2	0.0016887	−0.00031651	1.7242e-06
3	−0.00011195	1.0267e-05	−1.0534e-07
4	3.0478e-06	−1.776e-07	2.9975e-09
5	−4.1397e-08	1.6755e-09	−4.3294e-11
6	2.8014e-10	−8.0718e-12	3.0902e-13
7	−7.5246e-13	1.5353e-14	−8.6683e-16

TABLE 16

Values of coefficients $c_0^{2,2,m}$, $c_1^{2,2,m}$and $c_2^{2,2,m}$ for $b_{2,m}^2$ of equation (94) in case of a_2^2 of u_2 of equation (92)

m	$c_0^{2,2,m}$	$c_1^{2,2,m}$	$c_2^{2,2,m}$
0	−0.1208	−0.0018073	−7.7431e-05
1	0.039712	0.00099445	2.2037e-05
2	−0.0039312	−0.00012817	−2.1388e-06
3	0.00017579	6.5734e-06	9.7426e-08
4	−4.0495e-06	−1.669e-07	−2.3253e-09
5	5.0716e-08	2.2341e-09	3.0006e-11
6	−3.2704e-10	−1.512e-11	−1.9832e-13
7	8.496e-13	4.0796e-14	5.2636e-16

TABLE 17

Values of coefficients $c_0^{2,3,m}$, $c_1^{2,3,m}$and $c_2^{2,3,m}$ for $b_{3,m}^2$ of equation (94) in case of a_3^2 of u_2 of equation (92)

m	$c_0^{2,3,m}$	$c_1^{2,3,m}$	$c_2^{2,3,m}$
0	0.02176	0.0005804	9.4104e-06
1	−0.0067089	−0.00020457	−2.5829e-06
2	0.0006556	2.156e-05	2.4395e-07
3	−2.966e-05	−9.9711e-07	−1.0876e-08
4	6.9633e-07	2.3723e-08	2.5604e-10
5	−8.7919e-09	−3.0371e-10	−3.2742e-12
6	5.6633e-11	1.9905e-12	2.15e-14
7	−1.462e-13	−5.2428e-15	−5.6776e-17

TABLE 18

Values of coefficients $c_0^{3,0,m}$, $c_1^{3,0,m}$ and $c_2^{3,0,m}$ for $b_{0,m}^3$ of equation (94) in case of a_0^3 of u_3 of equation (92)

m	$c_0^{3,0,m}$	$c_1^{3,0,m}$	$c_2^{3,0,m}$
0	−0.046298	−0.0057663	−0.00018642
1	0.01272	0.0017156	4.8813e-05
2	−0.0010278	−0.0001572	−4.0434e-06
3	3.4667e-05	6.2343e-06	1.5655e-07
4	−6.1228e-07	−1.3209e-07	−3.2237e-09
5	5.8573e-09	1.5529e-09	3.65e-11
6	−2.9595e-11	−9.5349e-12	−2.1505e-13
7	6.2019e-14	2.3843e-14	5.1597e-16

TABLE 19

Values of coefficients $c_0^{3,1,m}$, $c_1^{3,1,m}$ and $c_2^{3,1,m}$ for $b_{1,m}^3$ of equation (94) in case of a_1^3 of u_3 of equation (92)

m	$c_0^{3,1,m}$	$c_1^{3,1,m}$	$c_2^{3,1,m}$
0	−0.15558	−0.0042536	−9.7633e-05
1	0.047606	0.0017754	3.2832e-05
2	−0.0046542	−0.00020881	−3.4242e-06
3	0.00020312	1.0088e-05	1.6314e-07
4	−4.6089e-06	−2.4592e-07	−4.0092e-09
5	5.6717e-08	3.2014e-09	5.2747e-11
6	−3.5983e-10	−2.1241e-11	−3.5329e-13
7	9.2209e-13	5.6467e-14	9.4664e-16

TABLE 20

Values of coefficients $c_0^{3,2,m}$, $c_1^{3,2,m}$ and $c_2^{3,2,m}$ for $b_{2,m}^3$ of equation (94) in case of a_2^3 of u_3 of equation (92)

m	$c_0^{3,2,m}$	$c_1^{3,2,m}$	$c_2^{3,2,m}$
0	0.11087	0.0061252	5.7319e-05
1	−0.029622	−0.0017355	−1.5993e-05
2	0.0025942	0.00016036	1.5228e-06
3	−0.00010795	−6.8539e-06	−6.7714e-08
4	2.3816e-06	1.5498e-07	1.5828e-09
5	−2.8856e-08	−1.9149e-09	−2.0088e-11
6	1.8081e-10	1.2223e-11	1.3102e-13
7	−4.5761e-13	−3.1539e-14	−3.4402e-16

TABLE 21

Values of coefficients $c_0^{3,3,m}$, $c_1^{3,3,m}$ and $c_2^{3,3,m}$ for $b_{3,m}^3$ of equation (94) in case of a_3^3 of u_3 of equation (92)

m	$c_0^{3,3,m}$	$c_1^{3,3,m}$	$c_2^{3,3,m}$
0	−0.015838	−0.00071563	−6.1847e-06
1	0.0042926	0.00019142	1.6456e-06
2	−0.00039171	−1.6809e-05	−1.5321e-07
3	1.6946e-05	6.9046e-07	6.7237e-09
4	−3.8371e-07	−1.5112e-08	−1.5611e-10
5	4.6824e-09	1.8183e-10	1.9738e-12
6	−2.9185e-11	−1.1361e-12	−1.2841e-14
7	7.3004e-14	2.8813e-15	3.3644e-17

Attachment 1
to Annex 1

Radio-meteorological data required for the clear-air prediction procedure

1 Introduction

The clear-air prediction procedures rely on radio-meteorological data to provide the basic location variability for the predictions. These data are provided in the form of maps which are contained in this Attachment.

2 Maps of vertical variation of radio refractivity data and surface refractivity

For the global procedure, the clear-air radio-meteorology of the path is characterized for the continuous (long-term) interference mechanisms by the average annual value of ΔN (the refractive index lapse-rate over the first 1 km of the atmosphere) and for the anomalous (short-term) mechanisms by the time percentage, β_0%, for which the refractive gradient of the lower atmosphere is below −100 N-units/km. These parameters provide a reasonable basis upon which to model the clear-air propagation mechanisms described in § 2 of Annex 1. The value for average sea-level surface refractivity, N_0, is used for the calculation of the troposcatter model.

If local measurements are not available, these quantities may be obtained from the maps in the integral digital products supplied with this Recommendation in the supplement file R-REC-P.452-18-202310-I!!ZIP-E.zip. These digital maps were derived from analysis of a ten-year (1983-1992) global dataset of radiosonde ascents. The maps are contained in the files DN50.txt and N050.txt, respectively. The data are from 0º to 360º in longitude and from +90º to −90º in latitude, with a resolution of 1.5º in both latitude and longitude. The data are used in conjunction with the companion data files LAT.txt and LON.txt containing respectively the latitudes and longitudes of the corresponding entries (grid points) in the files DN50.txt and N050.txt. For a location different from the grid points, the parameter at the desired location can be derived by performing a bi-linear interpolation on the values at the four closest grid points, as described in Recommendation ITU-R P.1144.

Attachment 2
to Annex 1

Path profile analysis

1 Introduction

For path profile analysis, a path profile of terrain heights above mean sea level is required. The parameters that need to be derived from the path profile analysis for the purposes of the propagation models are given in Table 22.

2 Construction of path profile

Based on the geographical coordinates of the interfering (φ_t, ψ_t) and interfered-with (φ_r, ψ_r) stations, terrain heights (above mean sea level) along the great-circle path should be derived from a topographical database or from appropriate large-scale contour maps. The distance between profile points should as far as is practicable capture significant features of the terrain. Typically, a distance increment between 30 m and 1 km is appropriate. In general, it is appropriate to use longer distance increments for longer paths. The profile should include the ground heights at the interfering and interfered-with station locations as the start and end points. The following equations take Earth curvature into account where necessary, based on the value of a_e found in equation (6a).

Although equally-spaced profile points are considered preferable, it is possible to use the method with non-equally-spaced profile points. This may be useful when the profile is obtained from a digital map of terrain height contours. However, it should be noted that the Recommendation has been developed from testing using equally-spaced profile points; information is not available on the effect of non-equally-spaced points on accuracy.

For the purposes of this Recommendation the point of the path profile at the interferer is considered as point zero, and the point at the interfered-with station is considered as point *n*. The path profile therefore consists of *n* + 1 points. Figure 7 gives an example of a path profile of terrain heights above mean sea level, showing the various parameters related to the actual terrain.

FIGURE 7

Example of a (trans-horizon) path profile

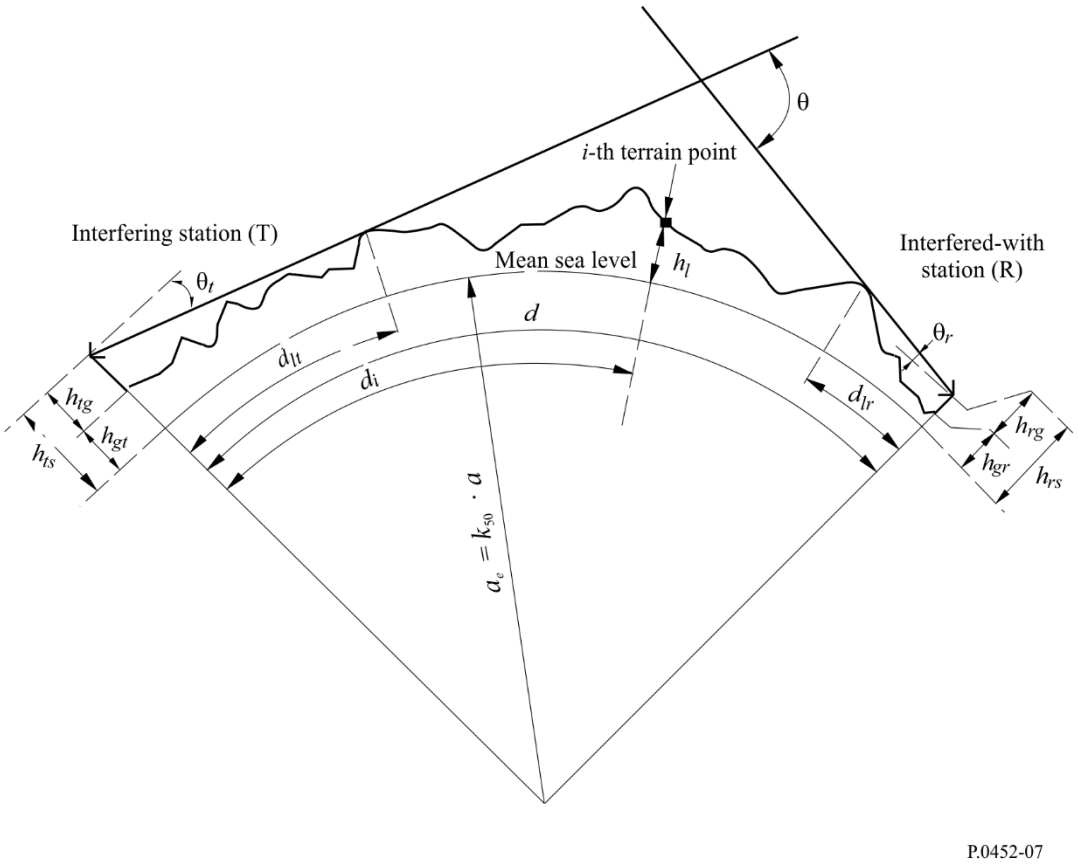

Note to Fig. 7: The value of θ_t as drawn will be negative.

Table 22 defines parameters used or derived during the path profile analysis.

TABLE 22

Path profile parameter definitions

Parameter	Description
a	Average physical Earth's radius (6 371 km)
a_e	Effective Earth's radius (km)
d	Great-circle path distance (km)
d_i	Great-circle distance of the *i*-th terrain point from the interferer (km)
d_{ii}	Incremental distance for regular path profile data (km)
f	Frequency (GHz)
λ	Wavelength (m)
h_{ts}	Interferer antenna height (m) above mean sea level (amsl)

TABLE 22 (*end*)

Parameter	Description
h_{rs}	Interfered-with antenna height (m) (amsl)
θ_t	For a transhorizon path, horizon elevation angle above local horizontal (mrad), measured from the interfering antenna. For a LoS path this should be the elevation angle toward the interfered-with antenna
θ_r	For a transhorizon path, horizon elevation angle above local horizontal (mrad), measured from the interfered-with antenna. For a LoS path this should be the elevation angle toward the interfering antenna
θ	Path angular distance (mrad)
h_{st}	Height of the smooth-Earth surface (amsl) at the interfering station location (m)
h_{sr}	Height of the smooth-Earth surface (amsl) at the interfered-with station location (m)
h_i	Height of the *i*-th terrain point amsl (m) h_0 : ground height of interfering station h_n : ground height of interfered-with station
h_m	Terrain roughness (m)
h_{te}	Effective height of interfering antenna (m)
h_{re}	Effective height of interfered-with antenna (m)

3 Path length

The path length can be obtained using great-circle geometry (based on the average physical Earth radius a) from the geographical coordinates of the interfering (φ_t, ψ_t) and interfered-with (φ_r, ψ_r) stations. Alternatively the path length can be found from a path profile. For general cases the path length, d (km), can be found from the path profile data:

$$d = \sum_{i=1}^{n} (d_i - d_{i-1}) \quad \text{km} \tag{134}$$

however, for regularly-spaced path profile data this simplifies to:

$$d = n \cdot d_{ii} \quad \text{km} \tag{135}$$

where d_{ii} is the incremental path distance (km).

4 Path classification

The path must be classified into LoS or transhorizon only for the determination of distances d_{lt} and d_{lr}, and elevation angles θ_t and θ_r, see below.

The path profile must be used to determine whether the path is LoS or transhorizon based on the median effective Earth's radius of a_e, as given by equation (6a).

A path is trans-horizon if the physical horizon elevation angle as seen by the interfering antenna (relative to the local horizontal) is greater than the angle (again relative to the interferer's local horizontal) subtended by the interfered-with antenna.

The test for the trans-horizon path condition is thus:

$$\theta_{max} > \theta_{td} \quad \text{mrad} \tag{136}$$

where:

$$\theta_{max} = \max_{i=1}^{n-1} (\theta_i) \quad \text{mrad} \tag{137}$$

θ_i: elevation angle to the *i*-th terrain point

$$\theta_i = 1000 \arctan\left(\frac{h_i - h_{ts}}{10^3 d_i} - \frac{d_i}{2\, a_e} \right) \quad \text{mrad} \tag{138}$$

where:

h_i: height of the *i*-th terrain point (m) amsl

h_{ts}: interferer antenna height (m) amsl

d_i: distance from interferer to the *i*-th terrain element (km).

$$\theta_{td} = 1000 \arctan\left(\frac{h_{rs} - h_{ts}}{10^3 d} - \frac{d}{2\, a_e} \right) \quad \text{mrad} \tag{139}$$

where:

h_{rs}: interfered-with antenna height (m) amsl

d: total great-circle path distance (km)

a_e: median effective Earth's radius appropriate to the path (equation (6a)).

5 Derivation of parameters from the path profile

5.1 Trans-horizon paths and LoS paths

The parameters to be derived from the path profile are those contained in Table 22.

5.1.1 Interfering antenna horizon elevation angle, θ_t

The interfering antenna's horizon elevation angle is the maximum antenna horizon elevation angle when equation (137) is applied to the $n - 1$ terrain profile heights.

$$\theta_t = \max(\theta_{max}, \theta_{td}) \quad \text{mrad} \tag{140}$$

with θ_{max} as determined in equation (137). Thus, for a LoS path the interfering antenna's horizon elevation angle is considered to be the elevation angle of the line to the interfered-with antenna.

5.1.2 Interfering antenna horizon distance, d_{lt}

The horizon distance is the minimum distance from the transmitter at which the maximum antenna horizon elevation angle is calculated from equation (137).

$$d_{lt} = d_i \quad \text{km} \quad \text{for max } (\theta_i) \tag{141}$$

For a LoS path, the index *i* should be the value which gives the maximum diffraction parameter ν:

$$\nu_{\max} = \max\left\{ \left[h_i + 500 C_e d_i (d - d_i) - \frac{h_{ts}(d - d_i) + h_{rs} d_i}{d} \right] \sqrt{\frac{0.002 d}{\lambda d_i (d - d_i)}} \right\} \tag{141a}$$

where the profile index i takes values from 1 to $n – 1$, and C_e is effective Earth curvature as defined in § 4.2.1 of Annex 1.

5.1.3 Interfered-with antenna horizon elevation angle, θ_r

The receive antenna horizon elevation angle is the maximum antenna horizon elevation angle when equation (137) is applied to the $n – 1$ terrain profile heights.

For a LoS path, θ_r is given by:

$$\theta_r = 1000 \arctan\left(\frac{h_{ts} - h_{rs}}{10^3 d} - \frac{d}{2a_e}\right) \quad \text{mrad} \tag{142a}$$

Otherwise, θ_r is given by:

$$\theta_r = \max_{j=1}^{n-1} (\theta_j) \quad \text{mrad} \tag{142b}$$

$$\theta_j = 1\,000 \arctan\left(\frac{h_j - h_{rs}}{10^3 (d - d_j)} - \frac{d - d_j}{2a_e}\right) \quad \text{mrad} \tag{143}$$

5.1.4 Interfered-with antenna horizon distance, d_{lr}

The horizon distance is the minimum distance from the receiver at which the maximum antenna horizon elevation angle is calculated from equation (142b).

$$d_{lr} = d - d_j \quad \text{km} \quad \text{for max } (\theta_j) \tag{144}$$

For a LoS path, d_{lr} is given by:

$$d_{lr} = d - d_{lt} \quad \text{km} \tag{144a}$$

5.1.5 Angular distance θ (mrad)

$$\theta = \frac{10^3\, d}{a_e} + \theta_t + \theta_r \quad \text{mrad} \tag{145}$$

5.1.6 "Smooth-Earth" model and effective antenna heights

5.1.6.1 General

A "smooth-Earth" surface is derived from the profile to calculate effective antenna heights both for the diffraction model, and for an assessment of path roughness required by the ducting/layer-reflection model. The definitions of effective antenna heights differ for these two purposes.

Section 5.1.6.2 describes the derivation of uncorrected smooth-earth surface heights at the transmitter and receiver, h_{st} and h_{sr} respectively.

Then § 5.1.6.3 describes the derivation of modified smooth-earth heights at the transmitter and receiver for the diffraction model, respectively h_{std} and h_{srd}, which in § 4.2.3 of Annex 1 are used to calculate the effective antenna heights for the diffraction model.

Section 5.1.6.4 describes the calculation of effective heights h_{te} and h_{re} and the terrain roughness parameter, h_m, for the ducting model.

5.1.6.2 Deriving the smooth-Earth surface

Derive a straight line approximation to the terrain heights (m) amsl of the form:

$$h_{si} = [(d - d_i)h_{st} + d_i h_{sr}]/d \quad \text{m} \tag{146}$$

where:

h_{si}: height (m) amsl, of the least-squares fit surface at distance d_i (km) from the interference source

h_{st}: height (m) amsl, of the smooth-Earth surface at the path origin, i.e. at the interfering station

h_{sr}: height (m) amsl, of the smooth-Earth surface at the path end, i.e. at the receiver station.

Evaluate h_{st} and h_{sr} as follows using equations (147) to (150):

$$v_1 = \sum_{i=1}^{n} (d_i - d_{i-1})(h_i + h_{i-1}) \tag{147}$$

where:

h_i: real height of the i-th terrain point (m) amsl

d_i: distance from interferer to the i-th terrain element (km).

$$v_2 = \sum_{i=1}^{n} (d_i - d_{i-1})[h_i(2d_i + d_{i-1}) + h_{i-1}(d_i + 2d_{i-1})] \tag{148}$$

The height of the smooth-Earth surface at the interfering station, h_{st}, is then given by:

$$h_{st} = \left(\frac{2v_1 d - v_2}{d^2} \right) \quad \text{m} \tag{149}$$

and hence the height of the smooth-Earth surface at the interfered-with station, h_{sr}, is given by:

$$h_{sr} = \left(\frac{v_2 - v_1 d}{d^2} \right) \text{m} \tag{150}$$

5.1.6.3 Smooth-earth surface heights for the diffraction model

Find the highest obstruction height above the straight-line path from transmitter to receiver h_{obs}, and the horizon elevation angles α_{obt}, α_{obr}, all based on flat-earth geometry, according to:

$$h_{obs} = \max_{i=1}^{n-1} \{H_i\} \quad \text{m} \tag{151a}$$

$$\alpha_{obt} = \max_{i=1}^{n-1} \{H_i / d_i\} \quad \text{mrad} \tag{151b}$$

$$\alpha_{obr} = \max_{i=1}^{n-1} \{H_i / (d - d_i)\} \quad \text{mrad} \tag{151c}$$

where:

$$H_i = h_i - [h_{ts}(d - d_i) + h_{rs} d_i] / d \quad \text{m} \tag{151d}$$

Calculate provisional values for the heights of the smooth surface at the transmitter and receiver ends of the path:

If h_{obs} is less than or equal to zero, then:

$$h_{stp} = h_{st} \quad \text{(m) amsl} \tag{152a}$$

$$h_{srp} = h_{sr} \quad \text{(m) amsl} \tag{152b}$$

otherwise:

$$h_{stp} = h_{st} - h_{obs}\, g_t \quad \text{(m) amsl} \tag{152c}$$

$$h_{srp} = h_{sr} - h_{obs}\, g_r \quad \text{(m) amsl} \tag{152d}$$

where:

$$g_t = \alpha_{obt} / (\alpha_{obt} + \alpha_{obr}) \tag{152e}$$

$$g_r = \alpha_{obr} / (\alpha_{obt} + \alpha_{obr}) \tag{152f}$$

Calculate final values for the heights of the smooth surface at the transmitter and receiver ends of the path as required by the diffraction model:

If h_{stp} is greater than h_0 then:

$$h_{std} = h_0 \quad \text{(m) amsl} \tag{153a}$$

otherwise:

$$h_{std} = h_{stp} \quad \text{(m) amsl} \tag{153b}$$

If h_{srp} is greater than h_n then:

$$h_{srd} = h_n \quad \text{(m) amsl} \tag{153c}$$

otherwise:

$$h_{srd} = h_{srp} \quad \text{(m) amsl} \tag{153d}$$

5.1.6.4 Parameters for the ducting/layer-reflection model

Calculate the smooth-Earth heights at transmitter and receiver as required for the roughness factor given by:

$$h_{st} = \min (h_{st}, h_0) \quad \text{m} \tag{154a}$$

$$h_{sr} = \min (h_{sr}, h_n) \quad \text{m} \tag{154b}$$

If either or both of h_{st} or h_{sr} were modified by equation (154a) or (154b) then the slope, m, of the smooth-Earth surface must also be corrected:

$$m = \frac{h_{sr} - h_{st}}{d} \quad \text{m/km} \tag{155}$$

The terminal effective heights for the ducting/layer-reflection model, h_{te} and h_{re}, are given by:

$$\begin{aligned} h_{te} &= h_{tg} + h_0 - h_{st} \quad \text{m} \\ h_{re} &= h_{rg} + h_n - h_{sr} \quad \text{m} \end{aligned} \tag{156}$$

The terrain roughness parameter, h_m (m) is the maximum height of the terrain above the smooth-Earth surface in the section of the path between, and including, the horizon points:

$$h_m = \max_{i = i_{lt}}^{i_{lr}} \left[h_i - (h_{st} + m \cdot d_i) \right] \quad \text{m} \tag{157}$$

where:

i_{lt}: index of the profile point at distance d_{lt} from the transmitter

i_{lr}: index of the profile point at distance d_{lr} from the receiver.

The smooth-Earth surface and the terrain roughness parameter h_m are illustrated in Fig. 8.

FIGURE 8

An example of the smooth-Earth surface and terrain roughness parameter

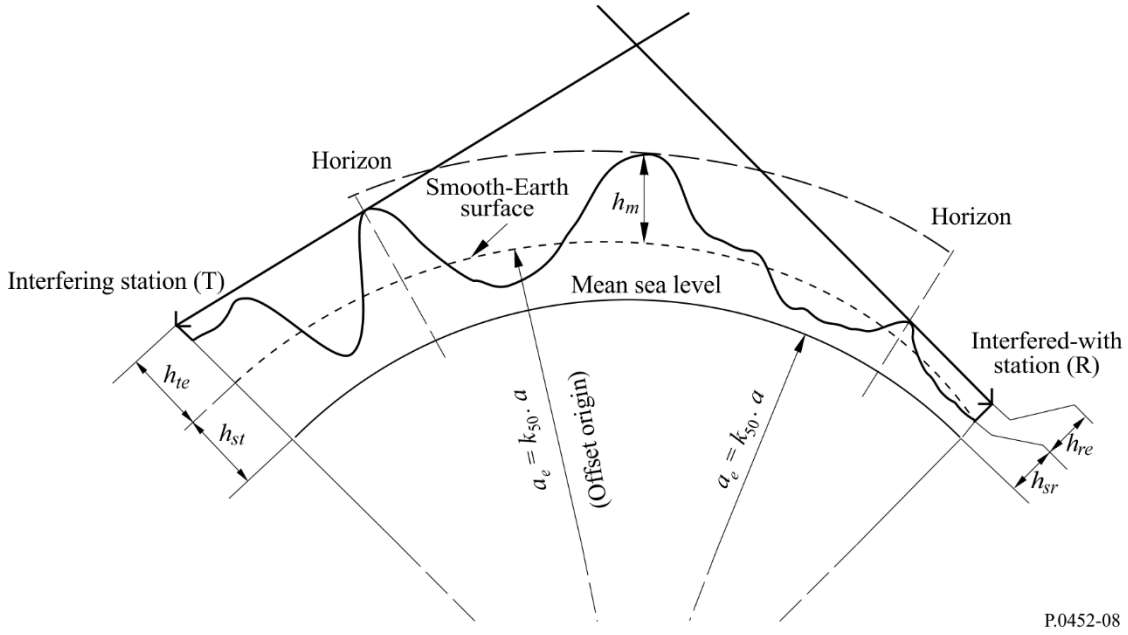

Attachment 3 to Annex 1

An approximation to the inverse cumulative normal distribution function for $x \leq 0.5$

The following approximation to the inverse cumulative normal distribution function is valid for $0.000001 \leq x \leq 0.5$ and is in error by a maximum of 0.00054. It may be used with confidence in the expression for the interpolation function in equation (41). If $x < 0.000001$, which implies $\beta_0 < 0.0001\%$, x should be set to 0.000001. The function $I(x)$ is then given by:

$$I(x) = \xi(x) - T(x) \tag{158}$$

where:

$$T(x) = \sqrt{[-2 \ln(x)]} \tag{158a}$$

$$\xi(x) = \frac{[(C_2 \cdot T(x) + C_1) \cdot T(x)] + C_0}{[(D_3 \cdot T(x) + D_2)\, T(x) + D_1] T(x) + 1} \tag{158b}$$

$$C_0 = 2.515516698 \quad (158c)$$

$$C_1 = 0.802853 \quad (158d)$$

$$C_2 = 0.010328 \quad (158e)$$

$$D_1 = 1.432788 \quad (158f)$$

$$D_2 = 0.189269 \quad (158g)$$

$$D_3 = 0.001308 \quad (158h)$$